

A Geometric Approach to the Kinematics of the Canfield Joint

Christian Bueno , Kristina V. Collins , Alan Hylton, and Robert Short 

Abstract—This paper details an accessible geometric derivation of the forward and inverse kinematics of a parallel robotic linkage known as the Canfield joint, which can be used for pointing applications. The original purpose of the Canfield joint was to serve as a human wrist replacement, and it can be utilized for other purposes such as the precision pointing and tracking of antennas, telescopes, and thrusters. We build upon previous analyses, and generalize them to include the situation where one of the three legs freezes; the kinematics are also substantially generalized beyond failure modes, detailed within. The core of this work states and clarifies the assumptions necessary to analyze this type of parallel robotic linkage. Specific guidance is included for engineering use cases.

I. INTRODUCTION

The Canfield joint is a parallel robotic linkage with three degrees of freedom (DoF) [1]. Originally designed to mimic a wrist joint, it has been explored for deep space optical communications [2], [3] and other end effectors, including solar cells and thrusters.

The Canfield joint bears some resemblance to a delta robot, but has a 3-RUR kinematic chain rather than a delta robot’s 3-RRR one.¹ The position and orientation of its distal plate, on which an end effector is mounted, is controlled entirely by three actuators, one at the base of each leg. Developed in 1997 [1], it is intended for use as a gimbal mechanism. Compared to a traditional three-axis concentric gimbal, the Canfield joint offers superior size, weight, and power (SWaP) characteristics: because of its parallel load paths, it can articulate a larger end effector mass than a gimbal of comparable size, and cables can be routed through its center, obviating the need for an additional cable tray.

The Canfield joint also offers a hemispherical workspace and robust pointing operation when reduced to two degrees of freedom. One of the key results of this paper is to elaborate on this robustness. In the event that one of the legs locks into place, such as due to motor failure, we show it is often still possible to precisely point at celestial objects. Along the way to this result, we solve other inverse kinematics problems and formalize, generalize, and simplify existing approaches. The robustness of the joint under this problem has been explored

Christian Bueno is in the Department of Mathematics, University of California, Santa Barbara, CA 93106. email: christianbueno@ucsb.edu

Kristina Collins is in the Department of Electrical, Computer, and Systems Engineering, Case Western Reserve University, Cleveland, Ohio, 44106 USA. email: kvc2@case.edu

Alan Hylton and Robert Short are with NASA Glenn Research Center, Cleveland, Ohio, 44135 USA. email: alan.g.hylton@nasa.gov, robert.s.short@nasa.gov

¹Here R, R, and U denote an actuated revolute joint, passive revolute joint, and passive universal joint respectively. See [4].

in prior work [5], [6], but we give a more precise and effective description for inverse kinematics here.

Despite being a parallel linkage, the Canfield joint has elegant kinematics when midplane symmetry is assumed. Given this assumption, we show it is possible to rigorously and completely solve various kinematic problems in a more general setting than previously addressed. In particular, the assumption of midplane symmetry enables us to study a generalized model of the Canfield joint which allows for variation of relative dimensions, including non-equilateral plates and unequal leg lengths. With the assumption of midplane symmetry, we can readily identify singularities of the forward kinematic mapping. Lastly, we demonstrate new relationships between quantities of interest and provide novel methods and visualizations.

II. MODEL CONSTRUCTION AND CONVENTIONS

To obtain rigorous results, we must first introduce a model of the Canfield joint as a spatial kinematic chain. We will do this in two steps: First we will introduce what we term a “half-joint” and second we define the Canfield joint as two half-joints glued together along their corresponding free ends.

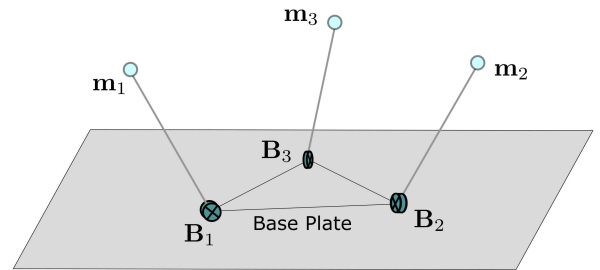


Fig. 1: Picture of a half-joint.

Definition. A **half-joint** is a triangular plate of nonzero area with links of nonzero length attached at each corner via a revolute joint (Figure 1). The free endpoints are termed **midjoints** and are denoted m_1 , m_2 , and m_3 .

Note that in the above definition, there is no restriction on how the revolute joint is oriented. Indeed its axis of rotation is free to be chosen, but fixed thereafter. This will lead to a substantial generalization of the mechanism introduced in [7].

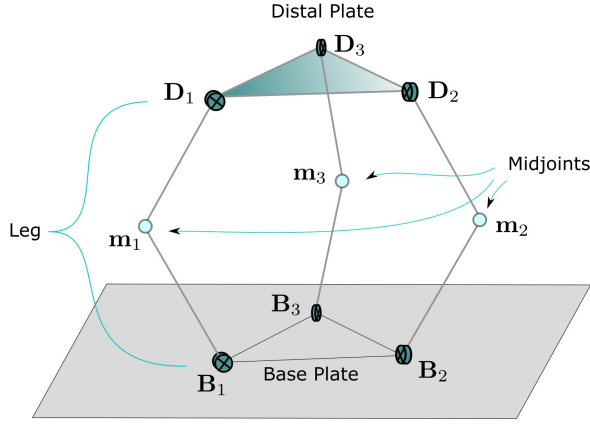


Fig. 2: Illustration of Canfield joint and variables.

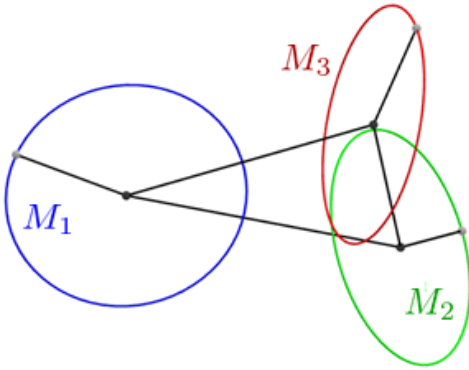


Fig. 3: Midcircles, relative to half-joint.

Definition. A **Canfield joint** consists of two identical half-joints attached at their corresponding midjoints via spherical² joints (Figure 2). We designate one of the half-joints as the **base half-joint** and refer to the other one as the **distal half-joint**.

- The **base plate (distal plate)**³ is the triangular plate on the base (distal) half-joint and the plane containing it is called the **base plane (distal plane)**.
- The **base hinges** and **distal hinges** are the revolute joints on the base plate and distal plate. Their locations are denoted by B_i and D_i for $i = 1, 2, 3$ respectively ordered counterclockwise and such that B_i and D_i corresponds to m_i . Only the base hinges are driven and we denote their axes of revolution by \hat{N}_i for $i = 1, 2, 3$ respectively.
- The i -th **midcircle** M_i is the circle of all possible positions for the midjoint m_i (Figure 3). The plane containing M_i is called the i -th **midcircle plane** and is denoted P_i .
- The **base normal** \hat{N}_B and **distal normal** \hat{N}_D are unit vectors normal to the base and distal planes respectively, such that the hinges are numbered in counter-clockwise order relative to said vector's orientation. Each can be

²The original prototype presented in [7] uses a universal joint which induces a slightly more restricted range of motion.

³Many implementations place the hinges on the lateral midpoints of the triangular plates instead of the corners. Nevertheless, these hinges will form a triangle and it's these hinge triangles which we call the base/distal plates.

concretely given by,

$$\hat{N}_B = \frac{(B_2 - B_1) \times (B_3 - B_1)}{\|(B_2 - B_1) \times (B_3 - B_1)\|}, \quad \hat{N}_D = \frac{(D_2 - D_1) \times (D_3 - D_1)}{\|(D_2 - D_1) \times (D_3 - D_1)\|}.$$

- The **base backward-normal** and **distal backward-normal** are respectively given by $-\hat{N}_B$ and $-\hat{N}_D$.

In this paper, the **base center** B_c is a distinguished point which can be located anywhere on the base plane. The **distal center** D_c is the point on the distal plane whose position relative to the distal hinges is the same as the base center's position relative to the base hinges (i.e. the point corresponding to B_c in the distal plane).⁴ We will give a simpler characterization of the distal center in Proposition III.1.

For this paper, any right-handed XYZ coordinate system with origin $B_c = \mathbf{0}$, z -direction $\hat{N}_D = \hat{z}$, and base plane as the XY plane, will suffice. For a more concrete coordinate system, we offer the following notion of a **base frame**: Let $\hat{x} := \frac{B_2 - B_1}{\|B_2 - B_1\|}$, $\hat{z} := \hat{N}_B$, and $\hat{y} := \hat{z} \times \hat{x}$. A **distal frame** can be defined analogously using the distal hinges and distal normal, but translated so that $D_c = \mathbf{0}$.

To simplify our analysis, we will allow different pieces of the mechanisms to intersect or even pass through one another. We also assume all the elements are infinitely thin. Since there are many ways to construct a Canfield joint, we leave it up to the end-user to discard solutions which are physically impossible or irrelevant for their use-case.

A Canfield joint model following the above definition requires three types of parameters to be specified: the distance from each hinge to its corresponding midjoint (denoted ℓ_i for $i = 1, 2, 3$), the distances between adjacent base hinges (denoted b_i for $i = 1, 2, 3$) and the orientation of the base hinge axes (introduced earlier as \hat{N}_i). This gives a total of $3 + 3 + 2 \cdot 3 = 12$ design parameters to be chosen. Using the above notations, we can describe the i -th midcircle M_i as the set of x satisfying the following constraints:

$$\begin{aligned} \hat{N}_i \cdot (x - B_i) &= 0, \\ \|x - B_i\|^2 &= \ell_i^2. \end{aligned}$$

Note that this level of generality is not taken in the construction established in [7]. In the **standard Canfield joint**, the base and distal plates are equilateral triangles, each hinge axis is parallel to the triangle side opposite said hinge, all the distances from a hinge to its connected midjoint are the same (denoted ℓ), and that the distances between any two adjacent hinges are the same (denoted b). In this simplified setup, it is typical to choose B_c to be the center of the base equilateral plate. The base hinge positions can then be given by:

$$B_1 = \frac{b}{\sqrt{3}} \hat{e}_1, \quad B_2 = \text{Rot}_z(\pi/3) B_1, \quad B_3 = \text{Rot}_z(\pi/3) B_2.$$

Where \hat{e}_1 is the standard basis vector in the X direction and $\text{Rot}_z(\theta)$ rotates vectors by angle θ with \hat{z} as the axis of rotation. To wit:

$$B_1 = \langle \frac{b}{\sqrt{3}}, 0, 0 \rangle, \quad B_2 = \langle -\frac{b}{2\sqrt{3}}, \frac{b}{2}, 0 \rangle, \quad B_3 = \langle -\frac{b}{2\sqrt{3}}, -\frac{b}{2}, 0 \rangle.$$

⁴In practice, the distal center is in the interior of the distal plate and is where the tool is located. However, we do not need to enforce such a restriction.

We will refer to this example on occasion throughout the paper. However, the results we have do not depend on this setup to proceed.

The core of our treatment is the following notion of midplane symmetry. We will use this idea throughout the paper.

Definition. A configuration of the Canfield joint has **midplane symmetry** if there is some plane passing through all three midjoints such that the reflection of the base half-joint over the the plane gives the distal half-joint. Such a plane is called the **midplane** for that configuration.

There are infinitely many planes that pass through all three midjoints if they are colinear. This can happen for certain design parameters, and can happen even in the case of the standard Canfield joint. However, if the configuration of the Canfield joint satisfies midplane symmetry, there is only one midplane for that configuration. Moreover, when the midjoints are not colinear, they may be used directly to uniquely identify the midplane. In this case, a normal vector to the midplane can be given by $\mathbf{N} = (\mathbf{m}_2 - \mathbf{m}_1) \times (\mathbf{m}_3 - \mathbf{m}_1)$.

Assuming midplane symmetry, specifying the base half-joint configuration and a plane through the midjoints determines a unique configuration of the Canfield joint with midplane symmetry. This unique configuration can be constructed by joining the base half-joint to its reflection across the provided plane. Conversely, given a configuration with midplane symmetry, the base half-joint configuration and midplane are uniquely determined (any two planes which cause the same reflection of the base half-joint must be the same). This correspondence allows us to focus on the midplane as an inverse kinematic tool which we informally describe below:

Midplane-symmetric Canfield joint configurations	\longleftrightarrow	Half-joint configurations equipped with a plane through midjoints
--	-----------------------	---

Although not every possible configuration of a Canfield joint will satisfy midplane symmetry, these are the only configurations we have seen reliably utilized in practice [7], [8], [9], [10], [5], [11]. Nevertheless, even with midplane symmetry, the cases where the midjoints are colinear allow for infinitely many choices of midplanes with which to complete the configuration. Such configurations are often associated with mechanical singularities that threaten a user's ability to control a Canfield joint. These are worth further study, as some configurations like these can be physically realized, however that is beyond the scope of this paper. Fortunately, these singularities seem to be rare and indeed, in [7], Canfield claimed that the eponymous mechanism had "A large, singularity free workspace." As such, we will assume the following:

Assumption. For the rest of this paper, we will assume that midplane symmetry is always satisfied by the configurations we are considering, unless otherwise stated.

III. FORWARD KINEMATICS

Since only the base angles are driven, we need a way of determining the entire configuration from this information alone, i.e. the forward kinematics. In [7], Canfield provides

a description of the forward kinematics which implicitly uses midplane symmetry in an essential way. We will make this assumption explicit as well as reformulate and generalize the forward kinematics.

Our first task is to unite the base angles and midjoints. The key to this are the midcircles M_1 , M_2 , and M_3 . As an example, in the standard Canfield joint constructed in [7], we can parametrize the midcircles using the base angles θ_1 , θ_2 , and θ_3 . Using this parametrization, we can locate the midjoints using the formulas below:

$$\begin{aligned}\mathbf{m}_1 &= \langle \ell \cos(\theta_1) + \frac{b}{\sqrt{3}}, 0, \ell \sin(\theta_1) \rangle, \\ \mathbf{m}_2 &= \langle -\frac{\ell}{2} \cos(\theta_2) - \frac{b}{2\sqrt{3}}, \frac{\ell\sqrt{3}}{2} \cos(\theta_2) + \frac{b}{2}, \ell \sin(\theta_2) \rangle, \\ \mathbf{m}_3 &= \langle -\frac{\ell}{2} \cos(\theta_3) - \frac{b}{2\sqrt{3}}, -\frac{\ell\sqrt{3}}{2} \cos(\theta_3) - \frac{b}{2}, \ell \sin(\theta_3) \rangle.\end{aligned}$$

Since we can define the midjoints in terms of the base angles, it suffices to phrase our remaining results in terms of just the midjoints. Detailed computations with specific values for ℓ_i , b_i , and $\hat{\mathbf{N}}_i$ are left to the interested reader.

Since we are assuming midplane symmetry, the distal half-joint must be the reflection of the base half-joint over the midplane. This will allow us to readily locate features of the distal half-joint. To simplify exposition, we introduce the following notation:

Notation. We use $R_P(\mathbf{a})$ to denote the reflection of a point \mathbf{a} over a plane P . If the plane P is given by $\mathbf{N} \cdot (\mathbf{x} - \mathbf{q}) = 0$ then we may use $R_{[\mathbf{N}, \mathbf{q}]}(\mathbf{a})$ to denote this reflection and it can be explicitly given by

$$R_P(\mathbf{a}) = R_{[\mathbf{N}, \mathbf{q}]}(\mathbf{a}) = \mathbf{a} - 2 \frac{\mathbf{N} \cdot (\mathbf{a} - \mathbf{q})}{\|\mathbf{N}\|^2} \mathbf{N}.$$

Remark 1. For convenience, we also note two special cases:

$$\begin{aligned}R_{[\mathbf{N}, \mathbf{0}]}(\mathbf{a}) &= \mathbf{a} - 2 \frac{\mathbf{N} \cdot \mathbf{a}}{\|\mathbf{N}\|^2} \mathbf{N}, \\ R_{[\mathbf{N}, \mathbf{q}]}(\mathbf{0}) &= 2 \frac{\mathbf{N} \cdot \mathbf{q}}{\|\mathbf{N}\|^2} \mathbf{N},\end{aligned}$$

and a consequence,

$$R_{[\mathbf{N}, \mathbf{q}]}(\mathbf{a} + \mathbf{b}) = R_{[\mathbf{N}, \mathbf{q}]}(\mathbf{a}) + R_{[\mathbf{N}, \mathbf{0}]}(\mathbf{b}).$$

Once the midplane has been defined, the distal half-joint is determined by reflecting the base plate over the midplane. This gives us the following proposition:

Proposition III.1 (Forward Kinematics). *If a configuration has midplane P which is normal to \mathbf{N} and contains \mathbf{q} , then*

$$\mathbf{D}_i = R_{[\mathbf{N}, \mathbf{q}]}(\mathbf{B}_i), \quad \mathbf{D}_c = R_{[\mathbf{N}, \mathbf{q}]}(\mathbf{0}), \quad \hat{\mathbf{N}}_D = R_{[\mathbf{N}, \mathbf{0}]}(-\hat{\mathbf{z}}).$$

We can choose $\mathbf{N} = (\mathbf{m}_2 - \mathbf{m}_1) \times (\mathbf{m}_3 - \mathbf{m}_1)$ and $\mathbf{q} = \mathbf{m}_i$ for any $i = 1, 2, 3$ if the midjoints are not colinear.

Proof. From definitions and midplane symmetry, we have that $R_P(\mathbf{B}_i) = \mathbf{D}_i$ and $R_P(\mathbf{B}_c) = R_P(\mathbf{0}) = \mathbf{D}_c$. This is what is meant by the phrase "the point corresponding to \mathbf{B}_c in the distal plane" in the definition of \mathbf{D}_c .

Next, note $\hat{\mathbf{N}}_D = (\hat{\mathbf{N}}_D + \mathbf{D}_c) - \mathbf{D}_c$ is normal to the distal plane. Thus, by reflection symmetry, $R_P(\hat{\mathbf{N}}_D + \mathbf{D}_c) - R_P(\mathbf{D}_c)$ is normal to the base plane. By the above, we know that

$R_P(\mathbf{D}_c) = \mathbf{B}_c = \mathbf{0}$, hence $R_P(\hat{\mathbf{N}}_D + \mathbf{D}_c)$ is normal to the base plane. By Remark 1 we have that

$$R_P(\mathbf{D}_c + \hat{\mathbf{N}}_D) = R_P(\mathbf{D}_c) + R_{[N,0]}(\hat{\mathbf{N}}_D) = R_{[N,0]}(\hat{\mathbf{N}}_D).$$

This must be $\pm\hat{\mathbf{z}}$ since the above is normal to the base plane and is also a unit vector (since $\hat{\mathbf{N}}_D$ was). Since reflections reverse orientations, the hinge numbering is now clockwise (instead of counter-clockwise) with respect to this vector. Thus, it is the case that $R_{[N,0]}(\hat{\mathbf{N}}_D) = -\hat{\mathbf{N}}_B = -\hat{\mathbf{z}}$. Applying $R_{[N,0]}$ to both sides yields $\hat{\mathbf{N}}_D = R_{[N,0]}(-\hat{\mathbf{z}})$.

Finally, the midplane must contain all the midjoints by definition and if the midjoints are not colinear, the midplane is normal $\mathbf{N} = (\mathbf{m}_2 - \mathbf{m}_1) \times (\mathbf{m}_3 - \mathbf{m}_1)$. \square

When the midjoints are not colinear, the midplane is uniquely determined and it is the one described in the above result. In this case, we can convert midjoints to a midplane and then get the distal features by reflection of base features. However, if the midjoints are colinear and the midplane is unknown, then the full configuration cannot be determined. This is a forward kinematic singularity which can be understood without appeal to traditional singularity analysis techniques involving Jacobians. Some examples of these singularities are discussed in [2]. Isolating and identifying the importance of the midplane symmetry assumption substantially clarifies why midjoint colinearity results in a breakdown of the forward kinematics described in [7].

Because the distal plate location is entirely determined by midplane reflection, there is no rotation component that might “twist” the distal plate relative to the base plate. The only possible exception is the theoretical and unrealistic case in which the distal center and base center are in the same place. Thus, any rotation required for assets on the distal plate needs to be attached and run independently to the Canfield joint.

A. Pointing the Distal Plate

Once we have the distal plate constructed, we should determine what objects can be pointed at by the configuration. To do so, we define some notions that will prove useful to us in the inverse kinematics construction.

Definition. The **forward-pointing ray** is the ray starting at the distal center which points along the distal normal and the **backward-pointing ray** has the same initial point but opposite direction. We say a configuration of a Canfield joint “**points at T** ” if the forward-pointing ray contains T and “**backward-points at T** ” if the backward-pointing ray contains T . The **pointing axis** is the union of these two rays.

If we have a configuration of the Canfield joint with midplane P , the pointing axis can be given by

$$\mathbf{r}(t) = \mathbf{D}_c + t\hat{\mathbf{N}}_D, \quad t \in \mathbb{R}$$

The forward-pointing ray is the pointing axis with $t \geq 0$, and the backward-pointing ray is the pointing axis with $t \leq 0$.

The following lemma gives us a means of connecting the forward-pointing ray to a construction based on the base half-joint which will prove useful in computing inverse kinematics.

Notation. Let Z denote the z -axis, $Z_{\geq 0}$ the non-negative side of the z -axis, and $Z_{\leq 0}$ the non-positive side of the z -axis in our chosen reference frame.

Lemma III.2 (Pointing Lemma). *A configuration of a Canfield joint with midplane P will point at T iff⁵ $R_P(\mathbf{T}) \in Z_{\leq 0}$. This holds for backward-pointing by replacing $Z_{\leq 0}$ with $Z_{\geq 0}$.*

Proof. Follows from definitions and midplane symmetry. The configuration points at T if and only if T is contained in its forward-pointing ray. By midplane symmetry, the midplane-reflection of $Z_{\leq 0}$ is the forward-pointing ray (and vice versa). It follows that the midplane reflection $R_P(\mathbf{T})$ lies in $Z_{\leq 0}$ if and only if T lies on the forward-pointing ray.

Analogously, midplane symmetry ensures the backward-pointing ray is the midplane reflection of $Z_{\geq 0}$ (and vice versa). Thus, by following an analogous proof we arrive at the Pointing Lemma with ‘point at’ replaced with ‘backward-point at’ and $Z_{\leq 0}$ replaced with $Z_{\geq 0}$. \square

IV. INVERSE KINEMATICS

Next we handle the inverse kinematics; a means of converting where we want the Canfield joint to point into base angles that achieve the pointing goal. In the context of a 2DoF gimbal, this pointing goal is typically expressed in terms of azimuth and elevation; in some cases, it may be expressed as a target point in XYZ space. In the case of the Canfield joint, however, constraining only the azimuth and elevation of the distal normal will result in an infinite number of solutions, as shown by the example illustrated in Figure 4. Thus, if we want finitely many solutions, we will need appropriate constraints, some of which we explore here and in Section V.

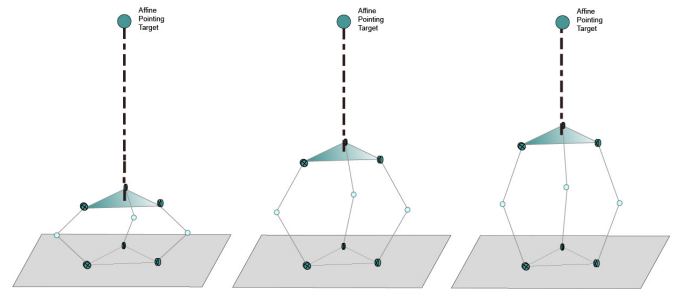
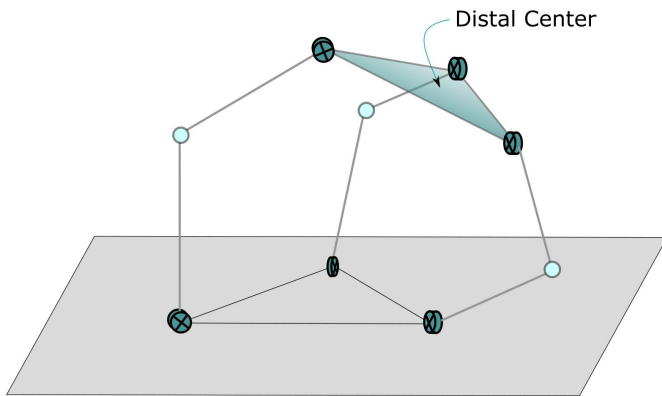


Fig. 4: Case of multiple configurations with the same pointing result.

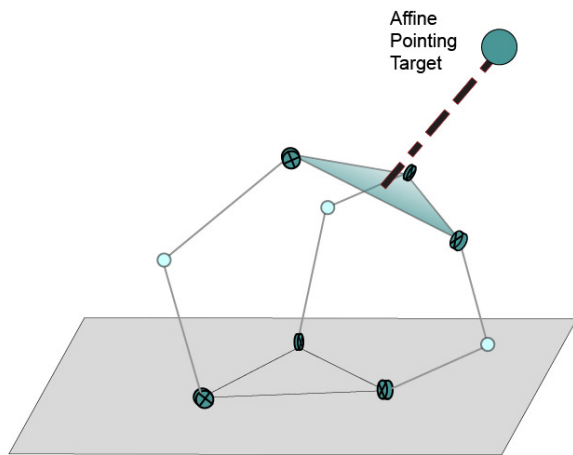
How we choose those constraints will change how the inverse kinematic solution is found. There are three main cases for inverse kinematics, shown in Figure 5:

- 1) **Distal Center (3DoF):** A position for the distal center is desired in XYZ space, without regard to orientation of the distal normal vector. This case is straightforward to derive. It may be desirable for a situation with a passively gimballed end effector, such as in additive manufacturing. This is illustrated in Figure 5a.

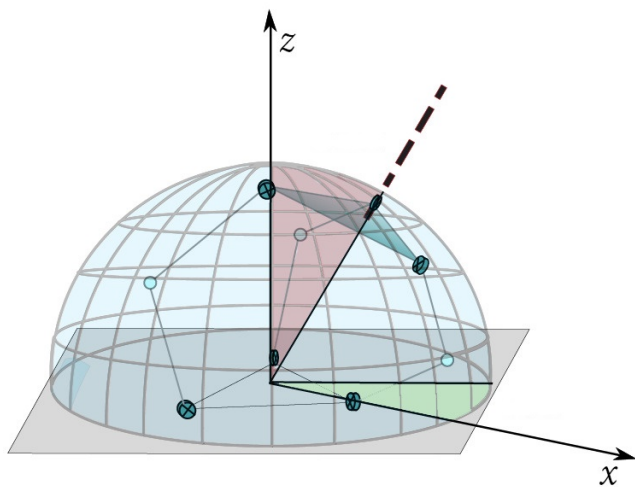
⁵The word iff is a standard contraction of “if and only if”.



(a) Inverse kinematics may be calculated for a given distal center location...



(b) ...or a point in 3-space that the configuration should point towards...



(c) ...or a direction in which the distal normal vector should point. NB: The positioning of the depicted configuration does not actually correspond to the distal normal depicted (see Theorem VI.1).

Fig. 5: Illustrations of inverse kinematics forms.

- 2) **Affine pointing (3DoF):** The end effector is directed to point at a desired point in XYZ space. This form may be desirable in laser machining, or for directing an instrument to point at a relatively near-field object. This is illustrated in Figure 5b.
- 3) **Az/EI Pointing (2DoF):** The Canfield joint is required to point in a certain direction, i.e. the distal normal has a prescribed orientation (often given in terms of azimuth and elevation, hence the name). This may be used in solar tracking [12], or for a survey telescope. This form is illustrated in Figure 5c. This provides a good approximation to affine pointing when targets are sufficiently far away.

Each of these three cases ultimately relies upon the inverse kinematic solution to a half-joint. Cases 2) and 3) have analogously defined backward-pointing versions as well. Since we are assuming midplane symmetry, we will be able to determine the solutions to these problems using simple geometric approaches.⁶

A. Distal Center to Midplane

Our first inverse kinematic form begins with a known location for the distal center. Once the location is known, there is a simple way to construct a midplane.

Theorem IV.1. A Canfield joint configuration has distal center $D_c \neq 0$ iff its midplane is given by

$$D_c \cdot (x - \frac{1}{2}D_c) = 0.$$

It has distal center $D_c = 0$ iff its midplane contains the origin.

Proof. By midplane symmetry, D_c is the reflection of the origin ($B_c = 0$) over the midplane. As such, $D_c - B_c = D_c$ is a normal vector to the midplane when $D_c \neq 0$. In addition, the distance from the origin to the midplane has to be the same as the distance from the midplane to D_c . Thus, a point on the midplane is given by $\frac{1}{2}D_c$. Thus, the midplane is $D_c \cdot (x - \frac{1}{2}D_c) = 0$. Conversely, this plane reflects B_c to D_c by construction.

If $D_c = 0$, then midplane reflection leaves 0 unchanged. This can happen only if 0 lies on the midplane. Conversely, planes containing 0 produces $D_c = 0$ via forward kinematics. \square

Remark 2. The case where $D_c = 0$ stands out as unusual since any plane passing through 0 can be used to construct a configuration of a Canfield joint with that distal center. As such, any distal normal can be achieved when $D_c = 0$. Thus, for any T there is a plane through the origin that points at it.

B. Affine Pointing to Midplane

Now we consider the second inverse kinematic form: pointing at a target T . As we did for the distal center, we determine the necessary and sufficient criterion to construct midplanes compatible with the objective.

⁶These geometric techniques are sometimes reminiscent of compass and straightedge constructions. As a result, we found them to be readily implementable in related software such as *Geogebra*.

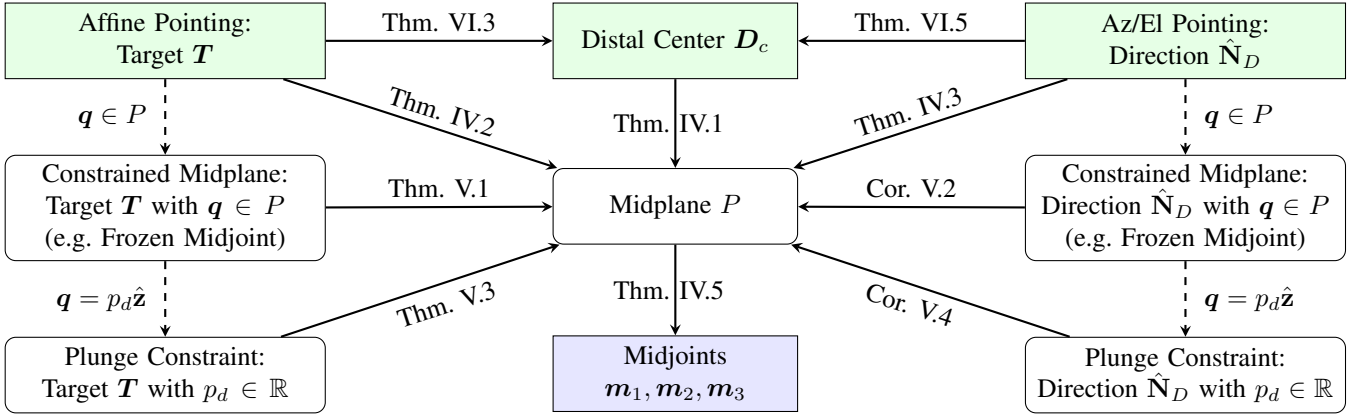


Fig. 6: A visual guide to the inverse kinematic. Dashed arrows indicate the introduction of a restriction. Solid arrows indicate inverse kinematics in direction of the arrow. Arrow labels reference the results in this paper corresponding to inverse kinematics of the arrow. Green boxes on the top row are starting positions and the blue box in the center bottom is the terminal position.

Theorem IV.2. A configuration with midplane P points at T iff $T \in P \cap Z_{\leq 0}$ or there exists $T \neq K \in Z_{\leq 0}$ such that P can be given by

$$(T - K) \cdot (x - \frac{T+K}{2}) = 0.$$

This holds for backward-pointing by replacing $Z_{\leq 0}$ with $Z_{\geq 0}$.

Proof. Let C be a configuration with midplane P . If C points at T , then by the Pointing Lemma III.2 $K := R_P(T) \in Z_{\leq 0}$. If $T \neq K$, then by symmetry, P orthogonally bisects the line segment \overline{TK} . Thus, P can be given by $(T - K) \cdot (x - \frac{T+K}{2}) = 0$. If $T = K$ then $R_P(T) = T$ which means $T \in P$. Thus $T \in P \cap Z_{\leq 0}$.

Conversely, suppose P satisfies the theorem's plane equation. Then it orthogonally bisects \overline{TK} for $K \in Z_{\leq 0}$ and so $R_P(T) = K \in Z_{\leq 0}$. Likewise, if $T \in P \cap Z_{\leq 0}$ then $R_P(T) = T \in Z_{\leq 0}$. Thus, either way, C points at T by the Pointing Lemma III.2.

The argument for backward-pointing is analogous and uses the backward-pointing version of the Pointing Lemma. \square

When $T \notin Z_{\leq 0}$, the above shows us there is a nice way to think of all the solution midplanes for pointing at T : they are orthogonal bisectors of line segments \overline{TK} where $K \in Z_{\leq 0}$.

C. Az/El Pointing to Midplane

Next we consider the third inverse kinematic form: pointing in direction \hat{N} , i.e. having distal normal $\hat{N}_D = \hat{N}$. As before, we solve for the midplane.

Theorem IV.3. A configuration has distal normal

- 1) $\hat{N}_D \neq -\hat{z}$ iff its midplane is orthogonal to $\hat{N}_D + \hat{z}$,
- 2) $\hat{N}_D = -\hat{z}$ iff its midplane is parallel to Z .

Holds for backward-normals by replacing \hat{N}_D with $-\hat{N}_D$.

Proof. Consider a configuration with midplane P given by $\hat{N} \cdot (x - q) = 0$. By the forward kinematics, the distal normal is given by $\hat{N}_D = R_{[\hat{N}, 0]}(-\hat{z}) = -\hat{z} + 2N_z\hat{N}$. Thus

$$\hat{N}_D + \hat{z} = 2N_z\hat{N}.$$

Observe that $\hat{N}_D = -\hat{z}$ iff $N_z = 0$ iff P is parallel to Z . On the other hand, $\hat{N}_D \neq -\hat{z}$ iff $N_z \neq 0$ iff $\hat{N}_D + \hat{z}$ and \hat{N} are non-zero scalar multiples. Thus $\hat{N}_D \neq -\hat{z}$ iff $\hat{N}_D + \hat{z}$ is normal to P .

The argument for the distal backward-normal is analogous and merely requires replacing \hat{N}_D with $-\hat{N}_D$. \square

Remark 3. We can write $\hat{N}_D = \sin \theta \hat{\rho} + \cos \theta \hat{z}$ where $\hat{\rho} \perp \hat{z}$ and θ is the smallest angle between \hat{N}_D and \hat{z} (the polar angle). Applying trigonometric identities we get that

$$\frac{\hat{N}_D + \hat{z}}{\|\hat{N}_D + \hat{z}\|} = \frac{\sin \theta \hat{\rho} + (1 + \cos \theta) \hat{z}}{\sqrt{2 + 2 \cos \theta}} = \sin\left(\frac{\theta}{2}\right) \hat{\rho} + \cos\left(\frac{\theta}{2}\right) \hat{z}.$$

Replacing the plane normal $\hat{N}_D + \hat{z}$ with $\sin\left(\frac{\theta}{2}\right) \hat{\rho} + \cos\left(\frac{\theta}{2}\right) \hat{z}$ in plane equations avoids numerical instability when $\hat{N}_D + \hat{z} \approx \mathbf{0}$. Similarly useful, we have $\frac{\hat{N}_D - \hat{z}}{\|\hat{N}_D - \hat{z}\|} = \cos\left(\frac{\theta}{2}\right) \hat{\rho} - \sin\left(\frac{\theta}{2}\right) \hat{z}$.

D. Midplane to Midjoints

As we saw in the past three subsections, we can find the associated midplanes for each of our three inverse kinematic forms. However, this does not form a complete solution to the inverse kinematic problem since we ultimately need to arrive at the base settings and not merely a midplane. In the following, we will see how to take a plane P and compute all possible base settings that can realize the plane P as a midplane. Or, if this is not possible, how to determine infeasibility.

Without loss of generality, we can work with the position of the midjoints instead of base angles since midjoint positions can be readily computed from the base angles and vice versa via trigonometry. For this reason, the Cartesian product of the midcircles $M := M_1 \times M_2 \times M_3$ captures all possible base half-joint settings.

Given a plane P which we wish to realize as a midplane, we will need to find where P intersects each midcircle M_i .

If P is given by $N \cdot (x - q) = 0$, this means solving for the midjoint m_i in the following system:

$$\begin{aligned} N \cdot (m_i - q) &= 0, \\ \hat{N}_i \cdot (m_i - B_i) &= 0, \\ \|m_i - B_i\|^2 &= \ell_i^2. \end{aligned}$$

Because each M_i is contained within its midcircle plane P_i , we have that either P is parallel to P_i or not. The following results deals first with the more difficult non-parallel case and then the simpler parallel cases.

Lemma IV.4. *Let P be a plane given by $N \cdot (x - q) = 0$. Suppose P is not parallel to the i -th midcircle plane P_i given by $\hat{N}_i \cdot (x - B_i) = 0$. Let q_i be some fixed point in the intersection of these two planes and $\delta_i = q_i - B_i$. Let $\nu_i = N \times \hat{N}_i$ and $\hat{\nu}_i = \frac{\nu_i}{\|\nu_i\|}$. Then, there exists a point in $P \cap M_i$ iff*

$$\Delta_i := (\hat{\nu}_i \cdot \delta_i)^2 - (\|\delta_i\|^2 - \ell_i^2) \geq 0.$$

Moreover, the i -th midjoint location(s) are given by

$$m_i = q_i - (\hat{\nu}_i \cdot \delta_i \pm \sqrt{\Delta_i}) \hat{\nu}_i.$$

If instead P is parallel to P_i but $P \neq P_i$, then $P \cap M_i = \emptyset$. If $P = P_i$, then $P \cap M_i = M_i$.

Proof. Suppose P is not parallel to P_i and let L_i be their line of intersection. Since $q_i \in L_i$ and $\hat{\nu}_i$ is a vector oriented parallel to L_i , we can parametrize L_i with the formula

$$L_i(t) := q_i + t\hat{\nu}_i, \quad t \in \mathbb{R}.$$

If $P \cap M_i$ is nonempty, then there must be some t for which $L_i(t) \in M_i$. Since all points of M_i are a distance ℓ_i from B_i this means

$$\begin{aligned} \ell_i^2 &= \|q_i + t\hat{\nu}_i - B_i\|^2 \\ &= \|q_i - B_i + t\hat{\nu}_i\|^2 \\ &= \|q_i - B_i\|^2 + \|\hat{\nu}_i\|^2 t^2 + 2t \hat{\nu}_i \cdot (q_i - B_i). \end{aligned}$$

Since $\delta_i = q_i - B_i$ and $\|\hat{\nu}_i\| = 1$ we have

$$t^2 + 2(\hat{\nu}_i \cdot \delta_i)t + (\|\delta_i\|^2 - \ell_i^2) = 0.$$

Using the quadratic formula to solve for t yields

$$t = -(\hat{\nu}_i \cdot \delta_i) \pm \sqrt{(\hat{\nu}_i \cdot \delta_i)^2 - (\|\delta_i\|^2 - \ell_i^2)}.$$

Thus, there will be solutions iff the discriminant $\Delta_i \geq 0$, and any member of $P \cap M_i$ will have the form

$$q_i - (\hat{\nu}_i \cdot \delta_i \pm \sqrt{\Delta_i}) \hat{\nu}_i.$$

Lastly, we consider what happens if P is parallel to P_i . If $P \neq P_i$, then P and P_i are disjoint so $P \cap M_i = \emptyset$. If $P = P_i$, then M_i is contained in P so $P \cap M_i = M_i$. \square

Remark 4. We can always choose q_i to be the orthogonal projection of q onto L_i , in which case it can be given explicitly as $q_i = q - \frac{\hat{N}_i \cdot (q - B_i)}{\hat{N}_i \cdot (N \times \hat{\nu}_i)} N \times \hat{\nu}_i$. It is immediate that $q_i \in L_i$ because $N \cdot (q_i - q) = 0$ and $\hat{N}_i \cdot (q_i - B_i) = 0$. Also $\hat{\nu}_i \cdot (q_i - q) = 0$ and that finishes the argument that q_i is the orthogonal projection of q .

From here, intersecting the candidate midplane with each midcircle will yield the compatible midjoint locations that could support the plane. Combining these intersections gives the full solution set.

Theorem IV.5. *Given a Canfield joint and a plane P , the set of all midjoint positions (m_1, m_2, m_3) where each $m_i \in P$ is given by*

$$(M_1 \cap P) \times (M_2 \cap P) \times (M_3 \cap P).$$

Each factor of the Cartesian product can be computed via Lemma IV.4 and the following are the only possibilities:

- 1) P intersects every midcircle and is not parallel to any midcircle plane. In this case the solution set is finite.
- 2) P intersects every midcircle but P is identical to some midcircle plane. In this case, the solution set is infinite.
- 3) P does not intersect one of the midcircles. In this case, the solution set is empty.

Proof. By definition of intersection, the set of midjoint position tuples is given by $(M_1 \cap P) \times (M_2 \cap P) \times (M_3 \cap P)$.

If we have $P \cap M_i \neq \emptyset$ and P is not parallel to P_i , then $P \cap M_i$ has at most two points by Lemma IV.4. If this happens for all i then the solution set is a Cartesian product of three sets of size at most 2, and is therefore a set of size at most 8.

If P is identical to some P_i , then $P \cap M_i = M_i$ which is infinite. If P intersects the other two midcircles, then the Cartesian product is a product of two nonempty sets and an infinite set. Thus, the solution set is infinite.

Lastly, if $P \cap M_i = \emptyset$ for some i , then we have a Cartesian product with one empty factor. Thus, the solution set is empty. \square

Even in case (1), there may be multiple solutions. In fact, case (1) can yield up to 8 different midjoint settings by reflecting m_i across the line between B_i and D_i (Figure 7). However, for both (1) and (2), physical restrictions can limit the number of solutions by making some points of $P \cap M_i$ unobtainable. It is up to the reader to incorporate their physical constraints appropriately and find a solution that suits their needs.

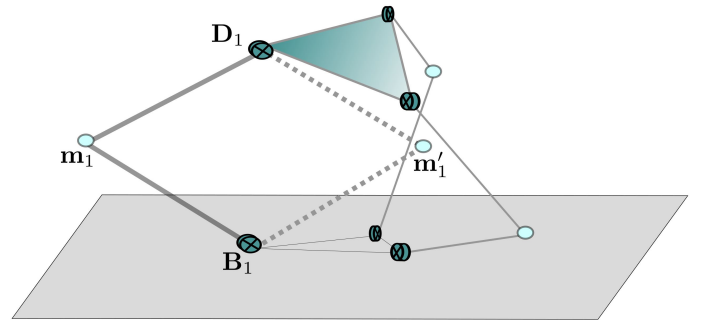


Fig. 7: For a given midplane, there may be 1, 2, 4, or 8 inverse kinematic solutions. Here, multiple solutions for one leg are shown.

V. CONSTRAINED KINEMATICS: FROZEN MIDJOINTS AND PLUNGE DISTANCE

In this section we consider the problem of pointing under additional constraints. Specifically, we will be constraining our Canfield joint by requiring that its midplanes always contain some prescribed fixed point \mathbf{q} . At first, this may seem artificial, but this arises naturally in two situations. The first is the popular plunge distance approach for controlling the Canfield joint in a gimbal-like manner. The second is a failure mode in which one of the midjoints is locked in place relative to the base plate due to its base hinge seizing up.

The former is well-known and introduced in Canfield's thesis [7]. The failure mode is less studied but has been discussed in [5] from a different perspective. It is particularly important to study in the context of deep space applications since repair may be impossible. One lesson from [5] is that despite the loss of a degree of freedom, it is still possible to point in a wide range of directions within the failure mode. However, in [5], we also see that maintaining a fixed plunge distance within the frozen midjoint failure mode unnecessarily limits the range of motion. As such, inverse kinematic solutions that do not depend on plunge distance are valuable in controlling the Canfield joint stuck in this failure mode.

In this section we shall provide exactly such a solution to the inverse kinematics of the frozen midjoint. We will also generalize the notion of plunge distance and extend the known inverse kinematics to these cases. Furthermore, we will unify the frozen midjoint and generalized plunge distance kinematics into one framework.

A. Constrained Midplane Inverse Kinematics

The following two results solve the affine and Az/El inverse kinematic problems for Canfield joints with midplanes constrained to contain a prescribed point \mathbf{q} .

Notation. We use $S_{(\mathbf{p},\mathbf{q})}$ to denote the sphere centered at \mathbf{p} that passes through point \mathbf{q} (where sphere means a ball's surface).

Theorem V.1. *Consider a Canfield joint constrained to have a fixed point \mathbf{q} in its midplane. Let C be a configuration of this constrained Canfield joint, P its midplane, and \mathbf{T} some target point. Then the following hold:*

- a) *If $\mathbf{T} \notin Z_{\leq 0}$, then C points at \mathbf{T} iff there exists a point $\mathbf{K} \in S_{(\mathbf{q},\mathbf{T})} \cap Z_{\leq 0}$ so that P can be given by*

$$(\mathbf{T} - \mathbf{K}) \cdot (\mathbf{x} - \mathbf{q}) = 0.$$

- b) *If $\mathbf{T} \in Z_{\leq 0}$, then C points at \mathbf{T} iff P contains both \mathbf{q} and \mathbf{T} , or P is given by $\hat{\mathbf{z}} \cdot (\mathbf{x} - \mathbf{q}) = 0$ where $q_z \leq \frac{1}{2}T_z$.*

For backward-pointing, replace every ' \leq ' with ' \geq '.

Proof. Due to the midplane constraint, we can assume all midplanes have the form $\mathbf{N} \cdot (\mathbf{x} - \mathbf{q}) = 0$ for some $\mathbf{N} \neq \mathbf{0}$.

- a) Consider $\mathbf{T} \notin Z_{\leq 0}$. Assume there is a $\mathbf{K} \in S_{(\mathbf{q},\mathbf{T})} \cap Z_{\leq 0}$. Note that $\mathbf{T} \neq \mathbf{K}$ since $\mathbf{T} \notin Z_{\leq 0}$ and that $\mathbf{T} \in S_{(\mathbf{q},\mathbf{T})}$. Let P be the plane given by $(\mathbf{T} - \mathbf{K}) \cdot (\mathbf{x} - \mathbf{q}) = 0$. Since $\mathbf{T} - \mathbf{K} \neq \mathbf{0}$ is orthogonal to P and both $\mathbf{T}, \mathbf{K} \in S_{(\mathbf{q},\mathbf{T})}$, it follows that $R_P(\mathbf{T}) = \mathbf{K}$. Since $\mathbf{K} \in Z_{\leq 0}$, by the Pointing Lemma III.2, we have that C points at \mathbf{T} .

Conversely, if C points at \mathbf{T} , then by the Pointing Lemma III.2, $R_P(\mathbf{T}) \in Z_{\leq 0}$. Let $\mathbf{K} = R_P(\mathbf{T})$ and note that $\mathbf{T} - \mathbf{K} \neq \mathbf{0}$ is orthogonal to P . Additionally, $\|\mathbf{q} - \mathbf{T}\| = \|\mathbf{q} - \mathbf{K}\|$ since $\mathbf{q} \in P$. Thus $\mathbf{K} \in S_{(\mathbf{q},\mathbf{T})}$ and so $\mathbf{K} \in S_{(\mathbf{q},\mathbf{T})} \cap Z_{\leq 0}$. Thus P is given by $(\mathbf{T} - \mathbf{K}) \cdot (\mathbf{x} - \mathbf{q}) = 0$.

- b) Consider $\mathbf{T} \in Z_{\leq 0}$. If $\mathbf{q}, \mathbf{T} \in P$, then $R_P(\mathbf{T}) = \mathbf{T} \in Z_{\leq 0}$. If P is given by $\hat{\mathbf{z}} \cdot (\mathbf{x} - \mathbf{q}) = 0$ where $q_z \leq \frac{1}{2}T_z$, then since $\mathbf{T} = T_z \hat{\mathbf{z}}$ we have

$$R_P(\mathbf{T}) = R_{[\hat{\mathbf{z}},\mathbf{q}]}(\mathbf{T}) = T_z \hat{\mathbf{z}} - 2(T_z - q_z) \hat{\mathbf{z}} = (2q_z - T_z) \hat{\mathbf{z}}.$$

Since $q_z \leq \frac{1}{2}T_z$, we have $R_P(\mathbf{T}) \in Z_{\leq 0}$. Thus, either way, C points at \mathbf{T} by the Pointing Lemma III.2.

Conversely, if C points at \mathbf{T} , then $R_P(\mathbf{T}) \in Z_{\leq 0}$ by the Pointing Lemma III.2. If $\mathbf{T} \notin P$, then $\mathbf{T} \neq R_P(\mathbf{T})$. Since both $\mathbf{T}, R_P(\mathbf{T}) \in Z_{\leq 0}$, it follows that $\hat{\mathbf{z}}$ is normal to P . Thus, P must be given by $\hat{\mathbf{z}} \cdot (\mathbf{x} - \mathbf{q}) = 0$. By our above calculation, $R_P(\mathbf{T}) \in Z_{\leq 0}$ only if $q_z \leq \frac{1}{2}T_z$. On the other hand, if $\mathbf{T} \in P$ then P contains both \mathbf{q} and \mathbf{T} , as desired.

The backward-pointing version of the Pointing Lemma III.2 yields the analogous result which has every ' \leq ' replaced with ' \geq '. \square

Note that if $\mathbf{T} \in Z_{\leq 0}$ and there exists a different point $\mathbf{K} \in S_{(\mathbf{q},\mathbf{T})} \cap Z_{\leq 0}$, then $q_z \leq \frac{1}{2}T_z$ and $\mathbf{T} - \mathbf{K}$ is a multiple of $\hat{\mathbf{z}}$. Thus the procedure in a) correctly produces the plane $\hat{\mathbf{z}} \cdot (\mathbf{x} - \mathbf{q}) = 0$ from b). However, we can also choose $\mathbf{K} = \mathbf{T}$ as our point of intersection in $S_{(\mathbf{q},\mathbf{T})} \cap Z_{\leq 0}$. In this case $\mathbf{T} - \mathbf{K} = \mathbf{0}$, and so the provided plane equation breaks down. However, from b) we know that there are other solutions, and that they can be any plane containing both \mathbf{T} and \mathbf{q} . Thus when $\mathbf{T} \in Z_{\leq 0}$, we have *infinitely* many new solutions not captured by the technique in a). For this reason we broke this theorem into two cases: $\mathbf{T} \notin Z_{\leq 0}$ and $\mathbf{T} \in Z_{\leq 0}$. The first case being the most general, useful, and simplest to implement.⁷

Corollary V.2. *Consider a configuration with midplane P containing \mathbf{q} and with distal normal $\hat{\mathbf{N}}_D$. Then*

- 1) $\hat{\mathbf{N}}_D \neq -\hat{\mathbf{z}}$ iff P can be given by $(\hat{\mathbf{z}} + \hat{\mathbf{N}}_D) \cdot (\mathbf{x} - \mathbf{q}) = 0$.
- 2) $\hat{\mathbf{N}}_D = -\hat{\mathbf{z}}$ iff P is parallel to Z and $\mathbf{q} \in P$.

Holds for backward-normal by replacing $\hat{\mathbf{N}}_D$ with $-\hat{\mathbf{N}}_D$.

Proof. This follows immediately from Theorem IV.3 by adding the constraint that $\mathbf{q} \in P$. \square

B. Pointing with a Frozen Midjoint

Unless otherwise noted, we will assume that \mathbf{m}_1 is the frozen midjoint and denote it by $\mathbf{m}^* = \mathbf{m}_1$ since relabeling midjoints will yield analogous results. Freezing a midjoint at \mathbf{m}^* implies only considering midplanes that contain \mathbf{m}^* . Thus, the kinematics in this case is precisely that which we described in the previous subsection but with $\mathbf{q} = \mathbf{m}^*$.

As a result, Theorem V.1 and Corollary V.2 for $\mathbf{q} = \mathbf{m}^*$ solve pointing for this failure mode so long as we know the

⁷Note that to construct the plane in Theorem V.1a) we intersect spheres and rays, and then construct a plane through \mathbf{q} which is orthogonal to the line segment $\overline{\mathbf{T}\mathbf{K}}$. All these steps are very geometric and have a 3D compass and straight-edge flavor. Indeed, this result can be readily implemented in geometric software such as *GeoGebra*.

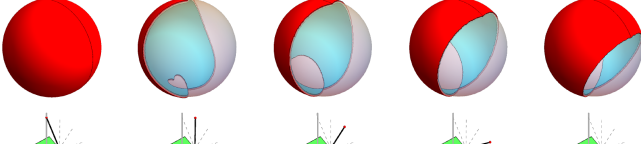


Fig. 8: A Standard Canfield joint with $b = \sqrt{3}$ and $\ell = 2$. Each column assumes a frozen midjoint and is analyzed as in Section VI-C. Bottom row: Position of frozen midjoint. Top row: Feasible distal normal orientations due to the frozen midjoint position (allowing self-intersection of the mechanism). The feasible region is painted red on the exterior surface and cyan on the interior surface; the unreachable part of the unit sphere is translucent.

location of the frozen midjoint \mathbf{m}^* . In practice, this amounts to knowing the base angle for the frozen midjoint, which is something that the user knows or can likely infer.

However, these theorems do not account for the geometry of the Canfield joint which can make some of the solutions geometrically impossible. To account for that, we would need to check whether the solution midplane intersects each midcircle. Using the result in Section IV-D we can answer these questions and in Section VI-C we show how to determine which distal normal orientations can be obtained (accounting for the the joint geometry). Figure 8 illustrates the pointing capabilities within 5 failure mode scenarios. Since distal normals are always unit vectors, they have a one-to-one correspondence to points on a unit sphere. For a given frozen midjoint configuration, shown in the second row, the set of distal normals which can be achieved are opaque on the sphere above it. Here we can see that there is still a large amount of accessible distal normal orientations despite having one midjoint locked in place. In Section V-D we will explain the extraordinary pointing capability exhibited in the leftmost example, where the set of achievable distal normals encompasses the entire sphere.

When applying Theorem V.1a) we need to check that the \mathbf{K} we find lies in $Z_{\leq 0}$. Since a sphere intersects a line in either 0, 1, or 2 locations, there can be up to 2 candidate midplanes in this case. It is straightforward to compute what \mathbf{K} is; we simply need to find the points on the sphere $\|\mathbf{K} - \mathbf{m}^*\|^2 = \|\mathbf{m}^* - \mathbf{T}\|^2$ with $K_x = K_y = 0$ and $K_z \leq 0$. Keeping mind that $K_z \leq 0$, this simplifies to solving

$$m_x^{*2} + m_y^{*2} + (K_z - m_z^*)^2 = \|\mathbf{m}^* - \mathbf{T}\|^2,$$

and so by the quadratic equation we have

$$K_z = m_z^* \pm \sqrt{\|\mathbf{m}^* - \mathbf{T}\|^2 - (m_x^{*2} + m_y^{*2})}.$$

We need to determine which (if any) of these two solutions yield $K_z \leq 0$.

The above instantly tells us that there is no way to point at \mathbf{T} whenever $\|\mathbf{m}^* - \mathbf{T}\|^2 < m_x^{*2} + m_y^{*2}$. Checking for when $K_z \leq 0$ introduces a further constraint. Thus the conditions

for \mathbf{T} that need to be satisfied for the existence of $\mathbf{K} \in Z_{\leq 0}$ are

$$\begin{aligned} \|\mathbf{m}^* - \mathbf{T}\|^2 &\geq m_x^{*2} + m_y^{*2}, & m_z^* &\leq 0, \\ \|\mathbf{m}^* - \mathbf{T}\|^2 &\geq \|\mathbf{m}^*\|^2, & m_z^* &\geq 0 \end{aligned}$$

Finally, once a midplane is determined, we can use Theorem IV.5 to find the midjoint positions for the non-frozen midjoints if they exist. For the Az/El problem, things are simpler and we just apply Corollary V.2 and Theorem IV.5 directly.

C. Pointing with a Fixed Plunge Distance

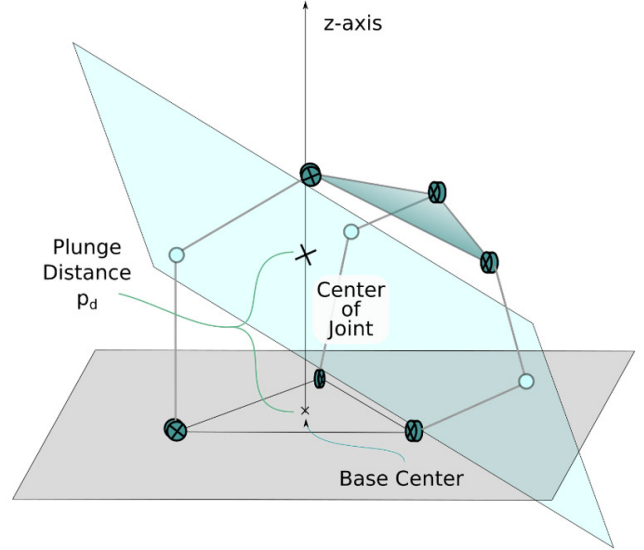


Fig. 9: Illustration of plunge distance.

In [7], the idea of the plunge distance is used to constrain the kinematics so that a standard Canfield joint can be effectively controlled. As such, we include this here for completeness and to provide our own more general definitions and results.

Definition. Given a Canfield joint configuration, we say it has **plunge distance** $p_d \in \mathbb{R}$ if the midplane intersects the Z axis at the point $\mathbf{c}_J = p_d \hat{\mathbf{z}}$. If the midplane does not intersect the Z axis, then we say $p_d = \infty$ (see Figure 10).⁸ If the Canfield joint is constrained to have plunge distance p_d , we call \mathbf{c}_J the **center** of the Canfield joint.

Remark 5. It is possible for the midplane to completely contain the Z axis. In these cases, the above definition implies every finite plunge distance is achieved simultaneously.

This definition naturally extends the one found in [7] by working for arbitrary choice of base center and allowing for zero, negative, and infinite plunge distances. As a result, this captures every way the midplane can intersect the Z axis. It is worth noting that plunge distance can potentially take on values outside the conventional range of $0 < p_d \leq \ell$. This

⁸There is no distinction between $-\infty$ and ∞ . We choose this because a midplane which doesn't intersect Z in \mathbb{R}^3 intersects Z at exactly one "point at infinity" in the projective geometry sense.

range has been embraced in past prototypes because it is well-suited to upward hemispherical pointing, but extending the plunge distance enables downward pointing with sufficiently long arms, as shown in Figure 13.

Next we show how to obtain the midplane for the affine pointing problem under a finite plunge distance constraint. In principle, we could simply apply Theorem V.1 with $\mathbf{q} = p_d \hat{\mathbf{z}}$ and get our solution. However, knowing the midplane intersects Z is a very special case and it will allow us to obtain very sharp result with extra effort. The following result handles every case except infinite plunge distance.

Theorem V.3. *Consider a Canfield joint constrained to have plunge distance $p_d \in \mathbb{R}$. Let C be a configuration of this constrained Canfield joint, P its midplane, and \mathbf{T} some target point. Then the following hold:*

a) *If $\mathbf{T} \notin Z_{\leq 0}$ and $\|\mathbf{T} - \mathbf{c}_J\| \geq |p_d|$, then C points at \mathbf{T} iff P is given by*

$$\left(\hat{\mathbf{z}} + \frac{\mathbf{T} - \mathbf{c}_J}{\|\mathbf{T} - \mathbf{c}_J\|} \right) \cdot (\mathbf{x} - \mathbf{c}_J) = 0$$

b) *If $\mathbf{T} \notin Z_{\leq 0}$ and $\|\mathbf{T} - \mathbf{c}_J\| \leq |p_d|$, then C points at \mathbf{T} iff and $p_d \leq 0$ and P is given by one of*

$$\left(\hat{\mathbf{z}} \pm \frac{\mathbf{T} - \mathbf{c}_J}{\|\mathbf{T} - \mathbf{c}_J\|} \right) \cdot (\mathbf{x} - \mathbf{c}_J) = 0$$

c) *If $\mathbf{T} \in Z_{\leq 0}$, then C points at \mathbf{T} iff P contains both \mathbf{c}_J and \mathbf{T} , or P is given by $\hat{\mathbf{z}} \cdot (\mathbf{x} - \mathbf{c}_J) = 0$ where $p_d \leq \frac{1}{2}T_z$.*

These hold for backward-pointing by replacing ‘ \leq ’ with ‘ \geq ’ wherever $Z_{\leq 0}$, $p_d \leq 0$, and $p_d \leq \frac{1}{2}T_z$ occur.

Proof. By the plunge constraint, we can assume all midplanes have the form $\mathbf{N} \cdot (\mathbf{x} - \mathbf{c}_J) = 0$ for some $\mathbf{N} \neq \mathbf{0}$ and $\mathbf{c}_J = p_d \hat{\mathbf{z}}$.

First assume $\mathbf{T} \in Z_{\leq 0}$. Part c) follows immediately by using Theorem V.1 for $\mathbf{q} = \mathbf{c}_J$ (and hence $q_z = p_d$).

Next assume $\mathbf{T} \notin Z_{\leq 0}$. Using Theorem V.1 for $\mathbf{q} = \mathbf{c}_J$, we know that C will point at \mathbf{T} iff there is a $\mathbf{K} \in S_{(\mathbf{c}_J, \mathbf{T})} \cap Z_{\leq 0}$ so that P can be given by $(\mathbf{T} - \mathbf{K}) \cdot (\mathbf{x} - \mathbf{c}_J) = 0$. Note that $\mathbf{K} \in S_{(\mathbf{c}_J, \mathbf{T})} \cap Z$ iff $\mathbf{K} = K_z \hat{\mathbf{z}}$ and

$$\|\mathbf{T} - \mathbf{c}_J\|^2 = \|\mathbf{K} - \mathbf{c}_J\|^2 = (K_z - p_d)^2.$$

Solving for K_z via the quadratic equation means

$$K_z = p_d \pm \|\mathbf{T} - \mathbf{c}_J\|.$$

Thus, C points at $\mathbf{T} \notin Z_{\leq 0}$ iff P can be given by

$$(\mathbf{T} - (p_d \pm \|\mathbf{T} - \mathbf{c}_J\|)\hat{\mathbf{z}}) \cdot (\mathbf{x} - \mathbf{c}_J) = 0,$$

and $p_d \pm \|\mathbf{T} - \mathbf{c}_J\| \leq 0$. Using $\mathbf{c}_J = p_d \hat{\mathbf{z}}$ and dividing both sides $\|\mathbf{T} - \mathbf{c}_J\|$ this plane equation can be rewritten as

$$\left(\frac{\mathbf{T} - \mathbf{c}_J}{\|\mathbf{T} - \mathbf{c}_J\|} \mp \hat{\mathbf{z}} \right) \cdot (\mathbf{x} - \mathbf{c}_J) = 0.$$

Now we tackle a) and b):

a) If we additionally assume $\|\mathbf{T} - \mathbf{c}_J\| \geq |p_d|$, then $-\|\mathbf{T} - \mathbf{c}_J\| \leq p_d \leq \|\mathbf{T} - \mathbf{c}_J\|$. From this we get $p_d - \|\mathbf{T} - \mathbf{c}_J\| \leq 0$ and $0 \leq p_d + \|\mathbf{T} - \mathbf{c}_J\|$, meaning $K_z = p_d - \|\mathbf{T} - \mathbf{c}_J\|$ is the only option. Thus, under this additional assumption, C points at \mathbf{T} iff P is given by

$$\left(\frac{\mathbf{T} - \mathbf{c}_J}{\|\mathbf{T} - \mathbf{c}_J\|} + \hat{\mathbf{z}} \right) \cdot (\mathbf{x} - \mathbf{c}_J) = 0.$$

b) If instead we additionally assume $\|\mathbf{T} - \mathbf{c}_J\| \leq |p_d|$, then both $0 \leq |p_d| \pm \|\mathbf{T} - \mathbf{c}_J\|$. If $p_d \geq 0$ then $|p_d| = p_d$, and then neither option yields $K_z \leq 0$. If $p_d \leq 0$, then $|p_d| = -p_d$ and this inequality becomes $0 \leq -p_d \pm \|\mathbf{T} - \mathbf{c}_J\|$, i.e. $0 \geq p_d \mp \|\mathbf{T} - \mathbf{c}_J\|$. Thus if $p_d \leq 0$, both choices lead to $K_z \leq 0$. Thus, under this additional assumption, C points at \mathbf{T} iff P is given by one of

$$\left(\frac{\mathbf{T} - \mathbf{c}_J}{\|\mathbf{T} - \mathbf{c}_J\|} \pm \hat{\mathbf{z}} \right) \cdot (\mathbf{x} - \mathbf{c}_J) = 0.$$

The backward-pointing version of the Pointing Lemma III.2 yields the analogous result. This results in replacing ‘ \leq ’ with ‘ \geq ’ wherever $Z_{\leq 0}$, $p_d \leq 0$, and $p_d \leq \frac{1}{2}T_z$ occur. \square

Obtaining the midplane for Az/EI pointing with constrained plunge distance is a simple application of our earlier efforts.

Corollary V.4. *Consider a configuration with midplane P , plunge distance $p_d \in \mathbb{R}$, and distal normal $\hat{\mathbf{N}}_D$. Then*

- 1) $\hat{\mathbf{N}}_D \neq -\hat{\mathbf{z}}$ iff P can be given by $(\hat{\mathbf{z}} + \hat{\mathbf{N}}_D) \cdot (\mathbf{x} - \mathbf{c}_J) = 0$.
- 2) $\hat{\mathbf{N}}_D = -\hat{\mathbf{z}}$ iff P contains Z .

Holds for backward-normal by replacing $\hat{\mathbf{N}}_D$ with $-\hat{\mathbf{N}}_D$.

Proof. Follows immediately from Corollary V.2 by letting $\mathbf{q} = \mathbf{c}_J = p_d \hat{\mathbf{z}}$ and observing that the only planes parallel to Z containing $p_d \hat{\mathbf{z}}$ are the planes containing Z itself. \square

Though the case of $p_d = \infty$ is omitted in the above results, we can quickly deduce that in that case the distal normal can only be $-\hat{\mathbf{z}}$. To see this, note that $p_d = \infty$ only if the midplane P is parallel to Z . Hence by midplane symmetry, $\hat{\mathbf{N}}_D = R_P(-\hat{\mathbf{z}}) = -\hat{\mathbf{z}}$. So only targets \mathbf{T} directly below the base plane can be pointed at when $p_d = \infty$, in which case the midplane must be given by $(\mathbf{T} - T_z \hat{\mathbf{z}}) \cdot (\mathbf{x} - \frac{\mathbf{T} + T_z \hat{\mathbf{z}}}{2}) = 0$.

One subtlety with plunge distance is that even with midplane symmetry, a finite plunge distance or well-defined center is not guaranteed. As an example of an undefined center, consider the configuration in Figure 10. Here, the midplane does not intersect the z -axis, so the plunge distance is ∞ and there is no center. Physical constructions of the Canfield joint, including the design of the original prototype [8], may restrict the range of motion of the base joints, and thereby the configuration space, such that configurations with vertical midplanes are impossible. However, such limitations will remove the ability to point straight down.

D. Pointing with a Frozen Midjoint and Fixed Plunge Distance

Finally, we revisit why one shouldn’t simply use the traditional plunge distance based kinematics when stuck in a frozen midjoint failure mode. Let P be a midplane of a Canfield joint configuration with frozen midjoint \mathbf{m}^* and finite plunge distance $p_d \in \mathbb{R}$. As we have seen, this means both \mathbf{m}^* and $\mathbf{c}_J = p_d \hat{\mathbf{z}}$ are on the midplane P . Additionally suppose $\mathbf{m}^* \neq \mathbf{c}_J$. Since $\mathbf{m}^* \in P$ and by midplane symmetry, \mathbf{m}^* must be equidistant to \mathbf{D}_c and $\mathbf{B}_c = \mathbf{0}$. Thus, $\mathbf{D}_c \in S_{(\mathbf{m}^*, \mathbf{0})}$. Similarly, \mathbf{c}_J is equidistant to \mathbf{D}_c and $\mathbf{B}_c = \mathbf{0}$, meaning $\mathbf{D}_c \in S_{(\mathbf{c}_J, \mathbf{0})}$. Thus $\mathbf{D}_c \in S_{(\mathbf{m}^*, \mathbf{0})} \cap S_{(\mathbf{c}_J, \mathbf{0})}$, i.e. the distal center is forced to lie on the intersection of two distinct spheres.

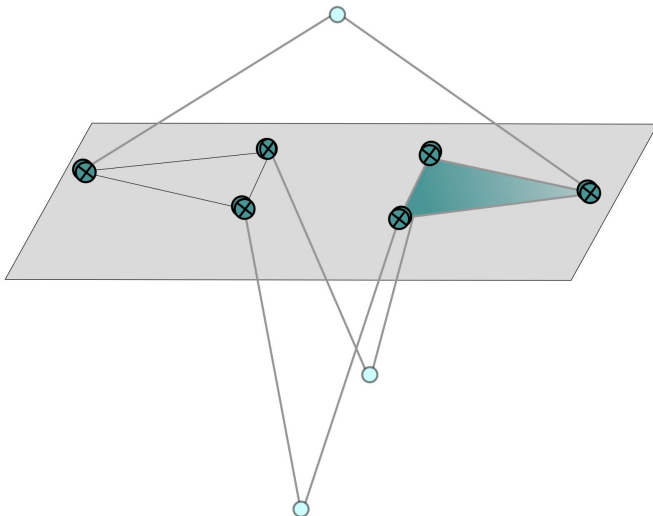


Fig. 10: A configuration with a vertical midplane and infinite plunge distance (the base triangle center is the base center).

The intersection of two distinct spheres is at best a circle. In practice, one can't even access all of this circle because the midplane-to-midjoint inverse kinematics further constrains what midplanes are viable. So we are working with some circular arc of possible distal centers. Thus by choosing to constrain the plunge distance while \mathbf{m}^* is frozen, we have severely limited our pointing abilities and have only 1DoF for moving the distal plate.

If by sheer coincidence \mathbf{m}^* lies on Z , then we can choose $p_d = \|\mathbf{m}^*\|$. In this case $\mathbf{c}_J = \mathbf{m}^*$ and the two spheres from before are identical. As a result, the intersection is an entire sphere and this means that D_c has 2 degrees of (spherical) freedom. In this very special case, nothing is lost by enforcing the correct plunge constraint. This can be seen in the leftmost example of Figure 8.

VI. ADDITIONAL CONSEQUENCES AND VISUALIZATIONS

In this section we explore some of the consequences of the inverse kinematics from previous section. In particular, we will introduce the distal normal field, the affine pointing locus, and the Az/El pointing locus. The loci may be used to solve the inverse kinematic problem, as shown in Figure 6, and provide a tool for visualization.

A. Distal Normal Field

A priori, to determine the distal normal we would need to know the midplane. However, Theorem IV.1 will allow us to determine the distal normals directly from nonzero distal centers because such distal centers determine their own midplane. This gives rise to a vector field $\mathbf{F}(\mathbf{x})$ which we call the **distal normal field**. It is given explicitly in the following theorem.

Theorem VI.1. *If a Canfield joint configuration has distal center $\mathbf{x} \neq \mathbf{0}$, then the distal normal is given by*

$$\mathbf{F}(\mathbf{x}) = 2 \frac{(\mathbf{x} \cdot \hat{\mathbf{z}})}{\|\mathbf{x}\|^2} \mathbf{x} - \hat{\mathbf{z}} = 2(\hat{\mathbf{x}} \cdot \hat{\mathbf{z}})\hat{\mathbf{x}} - \hat{\mathbf{z}}.$$

Moreover, for $\hat{\boldsymbol{\rho}} \perp \hat{\mathbf{z}}$

$$\mathbf{F}(\sin \theta \hat{\boldsymbol{\rho}} + \cos \theta \hat{\mathbf{z}}) = \sin 2\theta \hat{\boldsymbol{\rho}} + \cos 2\theta \hat{\mathbf{z}}.$$

Proof. For a point $\mathbf{x} \neq \mathbf{0}$ to be a distal center, the required midplane must be normal to \mathbf{x} and pass through $\mathbf{x}/2$ (Theorem IV.1). Thus, by Proposition III.1, the distal normal at \mathbf{x} is given by $R_{[\mathbf{x}, \mathbf{0}]}(-\hat{\mathbf{z}}) = -\hat{\mathbf{z}} + 2 \frac{(\mathbf{x} \cdot \hat{\mathbf{z}})}{\|\mathbf{x}\|^2} \mathbf{x}$ as desired. Finally, applying this formula with $\hat{\boldsymbol{\rho}} \perp \hat{\mathbf{z}}$,

$$\begin{aligned} \mathbf{F}(\sin \theta \hat{\boldsymbol{\rho}} + \cos \theta \hat{\mathbf{z}}) &= 2(\cos \theta \hat{\mathbf{z}})(\sin \theta \hat{\boldsymbol{\rho}} + \cos \theta \hat{\mathbf{z}}) - \hat{\mathbf{z}} \\ &= 2 \cos \theta \sin \theta \hat{\boldsymbol{\rho}} + (2 \cos^2 \theta - 1) \hat{\mathbf{z}} \\ &= \sin 2\theta \hat{\boldsymbol{\rho}} + \cos 2\theta \hat{\mathbf{z}}. \end{aligned}$$

□

Since $\hat{\mathbf{x}}$ is the normal to the midplane associated to \mathbf{x} ,⁹ the above shows that the distal normal doubles the polar angle. We visualize a 2D slice of this vector field in Figure 11 and note a resemblance to the magnetic field of a dipole.¹⁰

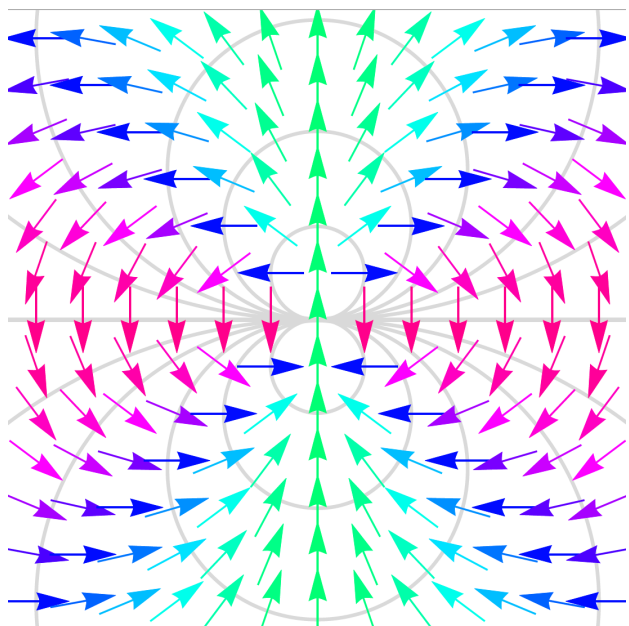


Fig. 11: 2D slice of $\mathbf{F}(\mathbf{x})$ on plane containing Z .

B. Pointing Loci: Pointing Constraint to Distal Center

If we want a Canfield joint to point at an object T (affine pointing), or in a direction N given by azimuth and elevation (Az/El pointing), there is a continuum of distal center locations that would get the job done. Here we will show how to find all the distal centers that accommodate such pointing objectives.

Definition. Given a target point T , let the **affine pointing locus** Λ_T be the set of distal centers D_c such that for some configuration $T = D_c + t\hat{N}_D$ for some $t \in \mathbb{R}$. The **affine forward-pointing locus** Λ_T^+ and **affine backward-pointing locus** Λ_T^- are the subset where $t \geq 0$ and $t \leq 0$ respectively.

⁹Where $\hat{\mathbf{x}} = \mathbf{x}/\|\mathbf{x}\|$ is not to be confused with the unit vector $\hat{\mathbf{x}}$.

¹⁰The magnetic field of a magnetic dipole with magnetic moment $\hat{\mathbf{z}}$ is given by $3(\hat{\mathbf{x}} \cdot \hat{\mathbf{z}})\hat{\mathbf{x}} - \hat{\mathbf{z}}$ times $\frac{\mu_0}{4\pi\|\mathbf{x}\|^3}$. Comparing to $\mathbf{F}(\mathbf{x}) = 2(\hat{\mathbf{x}} \cdot \hat{\mathbf{z}})\hat{\mathbf{x}} - \hat{\mathbf{z}}$ we can see that these two are nearly the same when ignoring the scalar factor.

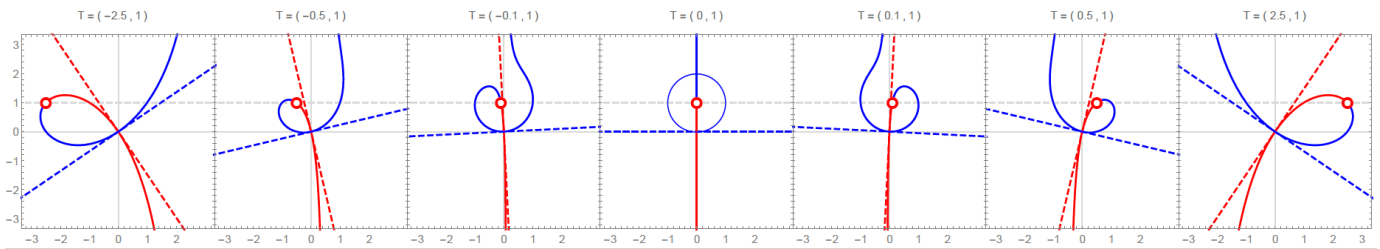


Fig. 12: The solid red, solid blue, dashed red, and dashed blue curves are $\Lambda_{\mathbf{T}}^+$, $\Lambda_{\mathbf{T}}^-$, $\tilde{\Lambda}_{\mathbf{N}}^+$, and $\tilde{\Lambda}_{\mathbf{N}}^-$ within W respectively. We set $\mathbf{T} = \mathbf{N}$ and depict \mathbf{T} with the hollow red dot. We vary T_ρ from -2.5 to 2.5 while keeping $T_z = 1$ fixed. Note the transition from a single curve to a union of a circle and line. Also note that the Az/El locus is tangent to the affine locus at the origin.

Remark 6. By this definition, $\mathbf{B}_c = \mathbf{0}$ is always in $\Lambda_{\mathbf{T}}$ because the origin can point anywhere (see Remark 2).

Simply put, $\Lambda_{\mathbf{T}}$ is the set of places the distal-center can be so that \mathbf{T} lies on the pointing axis of the configuration. This does not depend on a specific Canfield joint configuration and considers all possible Canfield joints at once.

The following result provides necessary and sufficient conditions for identifying elements of $\Lambda_{\mathbf{T}}$.

Theorem VI.2. Let $\mathbf{T} = T_\rho \hat{\rho} + T_z \hat{z}$ where $\hat{\rho} \perp \hat{z}$, and let $W = \text{span}\{\hat{\rho}, \hat{z}\}$ denote the ρz -plane. Then $W \cap \Lambda_{\mathbf{T}}$ is the set of points $\rho \hat{\rho} + z \hat{z}$ which satisfy the equation

$$E_{\mathbf{T}}(\rho, z) := \rho^3 + \rho z^2 + T_\rho(z^2 - \rho^2) - 2T_z \rho z = 0.$$

Moreover, if $\mathbf{T} \notin Z$ then

$$\Lambda_{\mathbf{T}} = \{\rho \hat{\rho} + z \hat{z} \mid E_{\mathbf{T}}(\rho, z) = 0\}.$$

Proof. By Remark 6 we know that $\mathbf{0} \in \Lambda_{\mathbf{T}}$, so assume $\mathbf{x} \neq \mathbf{0}$. Note that $\mathbf{x} \in W \cap \Lambda_{\mathbf{T}}$ iff we can write $\mathbf{x} = \rho \hat{\rho} + z \hat{z}$ and \mathbf{T} lies on the pointing axis of \mathbf{x} . By the Pointing Lemma III.2 and distal-center inverse kinematics, \mathbf{T} will lie on the pointing axis if and only if the plane through $\mathbf{x}/2$ is normal to \mathbf{x} (i.e. the midplane associated to \mathbf{x}) reflects \mathbf{T} onto the z -axis. This is equivalent to saying that $R_{[\mathbf{x}, \mathbf{x}/2]}(\mathbf{T})$ has no ρ -component, i.e.

$$0 = R_{[\mathbf{x}, \mathbf{x}/2]}(\mathbf{T}) \cdot \hat{\rho} = \left(\mathbf{T} - 2 \frac{(\mathbf{T} - \mathbf{x}/2) \cdot \mathbf{x}}{\|\mathbf{x}\|^2} \mathbf{x} \right) \cdot \hat{\rho}.$$

Multiplying by $\|\mathbf{x}\|^2$ and distributing the dot products, this is equivalent to

$$0 = T_\rho \|\mathbf{x}\|^2 - 2(\mathbf{T} \cdot \mathbf{x})\rho + \|\mathbf{x}\|^2 \rho,$$

which is the same as

$$0 = T_\rho(\rho^2 + z^2) - 2(T_\rho \rho + T_z z)\rho + (\rho^2 + z^2)\rho,$$

which when expanded reduces to $E_{\mathbf{T}}(\rho, z) = 0$.

Finally, if $\mathbf{T} \notin Z$ then $W = \text{span}\{\mathbf{T}, \hat{z}\}$. It follows from the Pointing Lemma III.2 that the pointing axis and z -axis must be reflections of each other over some plane. Hence these two lines must be coplanar. Since $\mathbf{T} \notin Z$ that means the plane containing the pointing axis and Z is the plane containing $\mathbf{0}$, \hat{z} , and \mathbf{T} which is W . Thus $\Lambda_{\mathbf{T}} \subseteq W$, so $\Lambda_{\mathbf{T}} \subseteq W \cap \Lambda_{\mathbf{T}}$. Since the reverse inclusion is automatic we have $\Lambda_{\mathbf{T}} = W \cap \Lambda_{\mathbf{T}}$. \square

Note that $\Lambda_{\mathbf{T}}$ does not depend on the design parameters ℓ_i , b_i , and $\hat{\mathbf{N}}_i$, and only depended on midplane symmetry and

that $\mathbf{B}_c = \mathbf{0}$. The next result lets us understand the geometry of the affine pointing locus and provides a parametrization.

Theorem VI.3. If $\mathbf{T} \in Z$ then $\Lambda_{\mathbf{T}} = Z \cup S_{(\mathbf{T}, \mathbf{0})}$. When $\mathbf{T} \notin Z$, then $\Lambda_{\mathbf{T}}$ is a planar nodal cubic curve passing through \mathbf{T} , with a node at $\mathbf{0}$, and can be rationally parametrized as

$$\mathbf{r}(t) = \left(\frac{\|\mathbf{T}\|^2 - t^2}{\|\mathbf{T} - t\hat{z}\|^2} \right) (\mathbf{T} - t\hat{z}), \quad t \in \mathbb{R}.$$

Moreover, $\Lambda_{\mathbf{T}}^+$ corresponds to $t \leq 0$, and $\Lambda_{\mathbf{T}}^-$ to $t \geq 0$.

Proof. If $\mathbf{T} \in Z$ then $T_\rho = 0$ and $\mathbf{T} = T_z \hat{z}$. Thus,

$$0 = E_{\mathbf{T}}(\rho, z) = \rho^3 + \rho z^2 - 2T_z \rho z = \rho(\rho^2 + (z - T_z)^2 - T_z^2).$$

This is zero iff $\rho = 0$ or $\rho^2 + (z - T_z)^2 = T_z^2$. By Theorem VI.2 and cylindrical symmetry, this means $\Lambda_{\mathbf{T}} = Z \cup S_{(\mathbf{T}, \mathbf{0})}$.

Now suppose $\mathbf{T} \notin Z$ and consider $t\hat{z} \in Z$ for $t \in \mathbb{R}$. By Theorem IV.2, the planes that point/backward-point at \mathbf{T} are precisely the ones normal to $\mathbf{N} = \mathbf{T} - t\hat{z}$ containing the midpoint $\mathbf{q} = \frac{1}{2}(\mathbf{T} + t\hat{z})$ for $t \leq 0$ and $t \geq 0$ respectively. The distal centers associated to these planes are given by

$$\mathbf{r}(t) = R_P(\mathbf{0}) = 2 \frac{\mathbf{N} \cdot \mathbf{q}}{\|\mathbf{N}\|^2} \mathbf{N} = \left(\frac{\|\mathbf{T}\|^2 - t^2}{\|\mathbf{T} - t\hat{z}\|^2} \right) (\mathbf{T} - t\hat{z}).$$

Thus, this curve is precisely $\Lambda_{\mathbf{T}}$ where $\Lambda_{\mathbf{T}}^+$ and $\Lambda_{\mathbf{T}}^-$ correspond to $t \leq 0$ and $t \geq 0$ respectively.

Finally, since $\mathbf{T} \notin Z$, we know $\Lambda_{\mathbf{T}}$ is a planar and given by a polynomial of third degree by Theorem VI.2. This cubic curve has a node at $\mathbf{0}$ because $\mathbf{r}(t) = \mathbf{0}$ has two solutions of $t = \pm \|\mathbf{T}\|$, but it is one-to-one everywhere else. \square

For Az/El pointing problems, we need a different pointing locus. We mimic the affine pointing locus results below.

Definition. Let $\mathbf{N} \neq \mathbf{0}$ and let $\hat{\mathbf{N}} = \frac{\mathbf{N}}{\|\mathbf{N}\|}$. The **Az/El forward-pointing locus** $\tilde{\Lambda}_{\mathbf{N}}^+$ is the set of distal centers where $\hat{\mathbf{N}}_D = \hat{\mathbf{N}}$ for some configuration. Similarly, the **Az/El backward-pointing locus** $\tilde{\Lambda}_{\mathbf{N}}^-$ is the set of distal centers where $\hat{\mathbf{N}}_D = -\hat{\mathbf{N}}$ for some configuration (i.e. the configuration has distal backward-normal $\hat{\mathbf{N}}$). Their union is the **Az/El pointing locus** $\tilde{\Lambda}_{\mathbf{N}} = \tilde{\Lambda}_{\mathbf{N}}^+ \cup \tilde{\Lambda}_{\mathbf{N}}^-$.

Remark 7. Note that $\tilde{\Lambda}_{-\mathbf{N}}^+ = \tilde{\Lambda}_{\mathbf{N}}^-$ and $\tilde{\Lambda}_{\alpha \mathbf{N}}^+ = \tilde{\Lambda}_{\mathbf{N}}^+$ for all $\alpha > 0$. So it will suffice to know $\tilde{\Lambda}_{\hat{\mathbf{N}}}^+$ for all unit vectors $\hat{\mathbf{N}}$.

Remark 8. A configuration with distal center \mathbf{x} and distal normal $\frac{\mathbf{N}}{\|\mathbf{N}\|}$ points at $\mathbf{x} + \mathbf{N}$ and backward-points at $\mathbf{x} - \mathbf{N}$.

As a result we can relate the Az/EI and affine pointing loci by: $\mathbf{x} \in \tilde{\Lambda}_N$ iff $\mathbf{x} \in \Lambda_{\mathbf{x}+N}$ when $N \neq \mathbf{0}$.

The following uses Theorem VI.2 and Remark 8 to give necessary and sufficient criteria for belonging to $\tilde{\Lambda}_N$.

Theorem VI.4. *Let $N = N_\rho \hat{\rho} + N_z \hat{z} \neq \mathbf{0}$ where $\hat{\rho} \perp \hat{z}$, and let $W = \text{span}\{\hat{\rho}, \hat{z}\}$ denote the ρz -plane. Then $W \cap \tilde{\Lambda}_N$ is the set of points $\rho \hat{\rho} + z \hat{z}$ given by*

$$\tilde{E}_N(\rho, z) := N_\rho(z^2 - \rho^2) - 2N_z \rho z = 0.$$

Moreover, if $N \notin Z$, then

$$\tilde{\Lambda}_N = \{\rho \hat{\rho} + z \hat{z} \mid \tilde{E}_N(\rho, z) = 0\}.$$

Proof. By Remark 8, we can deduce that $\mathbf{x} \in W \cap \tilde{\Lambda}_N$ iff $\mathbf{x} \in W \cap \Lambda_{\mathbf{x}+N}$. We know $\mathbf{x} \in W$ means $\mathbf{x} = \rho \hat{\rho} + z \hat{z}$ and so $\mathbf{x} + N = (\rho + N_\rho) \hat{\rho} + (z + N_z) \hat{z}$. This together with Theorem VI.2 tells us that $\mathbf{x} \in W \cap \Lambda_{\mathbf{x}+N}$ iff $\mathbf{x} = \rho \hat{\rho} + z \hat{z}$ and

$$0 = E_{\mathbf{x}+N}(\rho, z) = \rho^3 + \rho z^2 + (\rho + N_\rho)(z^2 - \rho^2) - 2(z + N_z)\rho z.$$

Simplifying this, we get the desired equation

$$0 = N_\rho(z^2 - \rho^2) - 2N_z \rho z.$$

Finally, if $N \notin Z$, then we can use a similar argument as in the proof of Theorem VI.2 to show that $\tilde{\Lambda}_N = W \cap \tilde{\Lambda}_N$. \square

Examining the graphs of the Az/EI pointing locus in Figure 12, we see it is composed of two lines. These are given by

$$N_\rho \rho + (N_z + \|N\|)z = 0, \quad N_\rho \rho + (N_z - \|N\|)z = 0.$$

when $N_\rho \neq 0$. We can check this by computing their product:

$$\begin{aligned} (N_\rho \rho + (N_z + \|N\|)z)(N_\rho \rho + (N_z - \|N\|)z) \\ = N_\rho^2(\rho^2 - z^2) + 2N_\rho N_z \rho z. \end{aligned}$$

Setting this to 0 and multiplying by -1 yields:

$$0 = N_\rho^2(z^2 - \rho^2) - 2N_\rho N_z \rho z = N_\rho \tilde{E}_N(\rho, z).$$

When $N_\rho \neq 0$, this is equivalent to $\tilde{E}_N(\rho, z) = 0$. Conveniently, one of these lines is the forward-pointing locus $\tilde{\Lambda}_N^+$ and the other is the backward-pointing locus $\tilde{\Lambda}_N^-$. Below, we shall give an alternate parametrization of these two lines.

Theorem VI.5. *Both $\tilde{\Lambda}_{-\hat{z}}^+$ and $\tilde{\Lambda}_{\hat{z}}^-$ are the base plane. For the other cases, $\tilde{\Lambda}_N^+$ and $\tilde{\Lambda}_N^-$ are orthogonal lines through the origin which can be parametrized respectively by*

$$\begin{aligned} \tilde{\mathbf{r}}^+(t) &= t \left(\hat{z} + \frac{N}{\|N\|} \right), \quad t \in \mathbb{R}, \quad \frac{N}{\|N\|} \neq -\hat{z}, \\ \tilde{\mathbf{r}}^-(t) &= t \left(\hat{z} - \frac{N}{\|N\|} \right), \quad t \in \mathbb{R}, \quad \frac{N}{\|N\|} \neq \hat{z}. \end{aligned}$$

Proof. By Theorem IV.3, a configuration has distal normal $-\hat{z}$ iff the midplane is parallel to Z . Forward kinematics implies such midplanes yield distal centers in the base plane. Thus $\tilde{\Lambda}_{-\hat{z}}^+ = \tilde{\Lambda}_{\hat{z}}^-$ is the base plane.

Next let $\hat{N} := \frac{N}{\|N\|} \neq -\hat{z}$. By Theorem IV.3, a configuration has distal normal $\hat{N} \neq -\hat{z}$ iff the midplane is orthogonal to $\hat{z} + \hat{N}$. Thus, midplanes for such configurations have midplanes of the form $(\hat{z} + \hat{N}) \cdot (\mathbf{x} - \mathbf{q}) = 0$ for some

\mathbf{q} . Forward kinematics implies such midplanes yield distal centers:

$$D_C = R_{[\hat{z} + \hat{N}, \mathbf{q}]}(\mathbf{0}) = 2 \frac{(\hat{z} + \hat{N}) \cdot \mathbf{q}}{\|\hat{z} + \hat{N}\|^2} (\hat{z} + \hat{N}).$$

Since \mathbf{q} was arbitrary, the coefficient of $(\hat{z} + \hat{N})$ can be any real number. Thus it follows $\tilde{\mathbf{r}}^+(t) = t(\hat{z} + \hat{N})$ parametrizes $\tilde{\Lambda}_N^+$. By Remark 7, we know $\tilde{\Lambda}_N^- = \tilde{\Lambda}_{-\hat{N}}^+$, so it follows that $\tilde{\mathbf{r}}^-(t) = t(\hat{z} - \hat{N})$ parametrizes $\tilde{\Lambda}_N^-$ for $\hat{N} \neq \hat{z}$. \square

The observant reader may notice that the two pointing loci equations are quite similar and in fact, they only differ by $\rho^3 + \rho z^2$ if we replace T_ρ and T_z with N_ρ and N_z respectively. Additionally, in Figure 12 we can see that for a given point \mathbf{T} , the lines tangent to $\Lambda_{\mathbf{T}}$ at the origin are precisely the lines given by $\tilde{\Lambda}_{\mathbf{T}}$. This is not a coincidence. One can show directly via projective geometry that $\Lambda_{\alpha \mathbf{T}} \rightarrow \tilde{\Lambda}_{\mathbf{T}}$ as $\alpha \rightarrow \infty$.¹¹ This can be interpreted as saying that the Az/EI locus becomes the affine locus when \mathbf{T} is infinitely far away. Alternatively, one can show this by computing tangent slopes using the results from Theorem VI.4 and Theorem VI.3.

C. Feasible Distal Normals for the Standard Canfield Joint

Let's consider a standard Canfield joint and recall that in this case we use the center of the equilateral base plate as the base center B_c . Moreover, since we are dealing with a standard Canfield joint, the midcircle planes P_i all intersect in a common line, namely Z .

In Section IV-D we describe how to obtain the midpoints from a midplane. In particular, Lemma IV.4 tells us that

$$\Delta_i = \left(\frac{\nu_i}{\|\nu_i\|} \cdot \delta_i \right)^2 - \|\delta_i\|^2 + \ell_i^2 \geq 0$$

is the necessary and sufficient criterion for determining whether a plane P given by $N \cdot (\mathbf{x} - \mathbf{q}) = 0$ will intersect M_i (assuming P is not parallel to P_i).

Multiplying both sides by $\|\nu_i\|^2$ and applying Lagrange's identity yields the constraint,

$$\|\nu_i\|^2 \Delta_i = \ell_i^2 \|\nu_i\|^2 - \|\nu_i \times \delta_i\|^2 \geq 0.$$

This condition is satisfied iff $\nu_i = \mathbf{0}$ or $\Delta_i \geq 0$.¹²

Recall that $\nu_i = N \times \hat{N}_i$ and $\delta_i = \mathbf{q}_i - B_i$ where \mathbf{q}_i is any point on $P \cap P_i$. We can replace ℓ_i with ℓ since all arm lengths are equal in a standard Canfield joint. Thus we obtain

$$\ell^2 \left\| N \times \hat{N}_i \right\|^2 - \left\| (N \times \hat{N}_i) \times (\mathbf{q}_i - B_i) \right\|^2 \geq 0,$$

and have such a constraint for each $i = 1, 2, 3$.

Now we will apply this to both the frozen midpoint failure mode and to the plunge constrained model with $p_d \in \mathbb{R}$. This means we assume P is given by $N \cdot (\mathbf{x} - \mathbf{q}) = 0$ where

¹¹In projective coordinates (also known as homogenous coordinates), $\alpha \mathbf{T}$ is given by $[\alpha T_\rho : \alpha T_z : 1] = [T_\rho : T_z : \frac{1}{\alpha}]$. The point at infinity obtained by taking $\alpha \rightarrow \infty$ is $\mathbf{T}^* := [T_\rho : T_z : 0]$. Extending $E_{\mathbf{T}} = 0$ to projective space (w.r.t \mathbf{T}) yields $T_w(\rho^3 + \rho z^2) + T_\rho(z^2 - \rho^2) - 2T_z \rho z = 0$ for points $[T_\rho : T_z : T_w]$. Plugging in \mathbf{T}^* yields $T_\rho(z^2 - \rho^2) - 2T_z \rho z = 0$ which is the Az/EI locus $\tilde{E}_{\mathbf{T}}(\rho, z) = 0$.

¹²Note $\nu_i = \mathbf{0}$ iff P is parallel to P_i . Since P_i contains Z , this means P is parallel to Z and so $\nu_i = \mathbf{0}$ implies $\hat{N}_D = -\hat{z}$ by Theorem IV.3.

$\mathbf{q} = \mathbf{m}^*$ or $\mathbf{q} = p_d \hat{\mathbf{z}}$. In the failure mode case, \mathbf{q}_i will be the projection of \mathbf{m}^* onto the line $P \cap P_i$ (see Remark 4). In the plunge case, \mathbf{q}_i can be chosen to be $p_d \hat{\mathbf{z}}$ for all i (because all P_i intersect at Z).

By Theorem VI.1 we know that the polar angle for $\hat{\mathbf{N}}_D$ is twice that of the polar angle of \mathbf{D}_c , and by Theorem IV.1 we also know that \mathbf{D}_c is a normal to the midplane (when $\mathbf{D}_c \neq \mathbf{0}$). Thus, in this assumed context, these results allow us to take a candidate distal normal $\hat{\mathbf{N}}_D = \sin \theta \hat{\rho} + \cos \theta \hat{\mathbf{z}}$, and produce the associated midplane $\hat{\mathbf{N}} \cdot (\mathbf{x} - \mathbf{q}) = 0$ where $\hat{\mathbf{N}} = \sin \frac{\theta}{2} \hat{\rho} + \cos \frac{\theta}{2} \hat{\mathbf{z}}$. Converting $\hat{\mathbf{N}}_D$ into $\hat{\mathbf{N}}$ and then testing with the above criteria for each $i = 1, 2, 3$, gives us a way of determining exactly which distal normals are achievable when accounting for the geometry of the base half-joint. If $\|\nu_i\|^2 \Delta_i \geq 0$ for all $i = 1, 2, 3$, then this distal normal is achievable. If even one fails, then it is not. Again note this takes into account the sizes of the midcircles.

Using this pipeline, we visualize pointing capabilities of plunge constrained standard Canfield joints for different choices of parameters in Figure 13. Similarly, we visualize the pointing capabilities of a standard Canfield joint in different frozen midjoint failure modes in Figure 8.

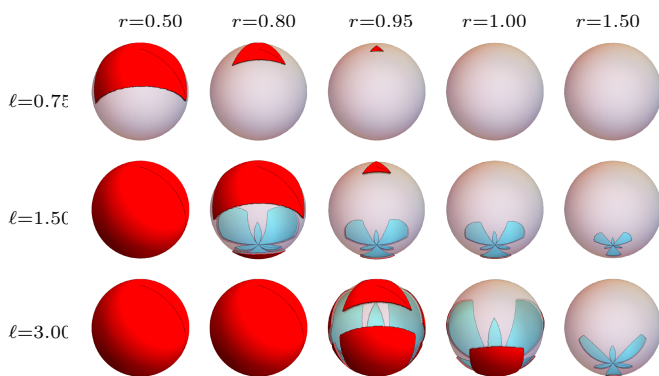


Fig. 13: Here ℓ is arm length, $p_d = r\ell$, and $b = \sqrt{3}$ (so the distance from \mathbf{B}_i to the base triangle center is 1). The covered regions of the sphere indicate which distal normal orientations are possible with those parameters (the color code is as in Figure 8). Note that when $r \geq 1$ (i.e. $p_d \geq \ell$), it is impossible to point up, but for sufficiently long arms it is still possible to point down. Also note that the ability to point down only appears after $\ell \geq 1$. As usual, this is under the assumption that the elements can pass through each other.

VII. FUTURE WORK

The foregoing presents the most general and rigorous kinematic analysis of the Canfield joint to date. This was in large part feasible due to the key assumption of midplane symmetry. However, it is known that this condition can be violated in special cases (see [2]). Thus, further research is warranted into what circumstances lead to loss of midplane symmetry and into what effect that may have on the kinematics. Such questions will require a thorough study of the full configuration space of the Canfield joint. To date, no such study has been conducted.

An additional reason to study the full configuration space of the Canfield joint is to shed light on its singularities. On the one hand, in line with the work in [7], we conjecture that the set of singular base settings is very small and specifically is of measure zero. On the other hand, empirical evidence suggest that even being near a singular configuration can prove deleterious in physical applications. Ideally, future investigations would lead to criteria by which dangerous base settings can be identified and avoided - either by software control or by adjusting the physical design of the Canfield joint. Conversely, dimensions and configurations of the Canfield joint may be designed to confer extraordinary pointing capability, as in the infinite plunge distance example shown in Figure 10, which holds promise for novel mechanisms.

Motion planning and control of a prototype Canfield joint was validated for the mission needs of a deep space optical communication use case, and the methods and results of this analysis will be discussed in a subsequent paper. However, the frozen midjoint case described above has not yet been integrated into motion planning algorithms for the Canfield joint or tested in a laboratory setting.

Finally, attention is also deserved by several concerns affecting physical robots which are not accounted for in this model: for example, the limitations of the physical midjoint linkages will limit the configuration space accessible to the robot and have important implications for future analysis of the dynamics.

REFERENCES

- [1] S. Canfield, C. Reinholtz, R. Salerno, and A. Ganino, "Spatial, parallel-architecture robotic carpal wrist," Dec. 23 1997, US Patent 5,699,695. [Online]. Available: <https://www.google.com/patents/US5699695>
- [2] K. V. Collins, "Towards a Canfield Joint for Deep Space Optical Communication," Master's thesis, Case Western Reserve University School of Graduate Studies, 2019. [Online]. Available: http://rave.ohiolink.edu/etdc/view?acc_num=case1536104606070327
- [3] K. Collins, D. Raible, and L. Burke, "Development and validation of a canfield joint as a precision pointing system for deep space instrumentation," submitted for publication.
- [4] H. D. Taghirad, *Parallel Robots: Mechanics and Control*. CRC Press, 2013.
- [5] R. Short and A. Hylton, "A Topological Kinematic Workspace Analysis of the Canfield Joint," *CoRR*, vol. abs/1809.02148, 2018. [Online]. Available: <http://arxiv.org/abs/1809.02148>
- [6] C. Bueno, "The Configuration Space and Kinematics of the Canfield Joint," 2019, poster presented at SIAM Conference on Applied Algebraic Geometry, Bern, Switzerland.
- [7] S. L. Canfield and C. F. Reinholtz, *Development of the carpal robotic wrist*. Berlin, Heidelberg: Springer Berlin Heidelberg, 1998, pp. 423–434. [Online]. Available: <https://doi.org/10.1007/BFb0112981>
- [8] A. Ganino, "Mechanical design of the carpal wrist: a parallel-actuated, singularity-free robotic wrist," Master's thesis, Virginia Tech, 2003.
- [9] J. Wrobel, R. Hoyt, J. Slostad, N. Storrs, J. Cushings, T. Moser, J. S. Luise, and G. Jimmerson, *PowerCube(TM) - Enhanced Power, Propulsion, and Pointing to Enable Agile, High-Performance CubeSat Missions*. AIAA, 2012. [Online]. Available: <https://arc.aiaa.org/doi/abs/10.2514/6.2012-5217>
- [10] L. Nguyen, S. Harris, V. Wang, and K. Duncan. (2015) Canfield joint. [Online]. Available: <https://sites.google.com/site/canfieldjoint/>
- [11] E. Bashevkin, J. Kenahan, B. Manning, B. Mahlstedt, and A. Kalman, "A novel hemispherical anti-twist tracking system (hatts) for cubesats," in *Proceedings of 26th Annual AIAA/USU Conference on Small Satellites*. Small Satellite Conf, 2012.
- [12] S. Canfield, "Developing Capture Mechanisms and High-Fidelity Dynamic Models for the MXER Tether System," 2007, nTRS 20080002099. [Online]. Available: <https://ntrs.nasa.gov/archive/nasa/casi.ntrs.nasa.gov/20080002099.pdf>